EVALUATION OF THE TIN-TUNGSTEN GREISEN MINERALIZATION AND ASSOCIATED GRANITE AT SLEITAT MOUNTAIN, SOUTHWESTERN ALASKA

By Roger E. Burleigh

Open-file report 35-91**********1991

UNITED STATES DEPARTMENT OF THE INTERIOR
Manuel J. Lujan, Jr., Secretary

BUREAU OF MINES
T S Ary, Director

CONTENTS

ILLUSTRATIONS

TABLES

APPENDIXES

UNIT OF MEASURE ABBREVIATIONS USED IN THIS REPORT

≈	approximately
ft^3	cubic feet
°	degree
ft	feet
<	less than
$\bar{x}$	mean (average)
$\bar{x} \pm \sigma$	mean plus or minus the standard deviation
mm	millimeter
Ma	millions of years before present
μm	micrometer
mi	mile
ppm	parts per million
%	percent
pct	percent
lbs	pounds
sec	second
st	short ton
ft^2	square feet
mi^2	square miles
σ	standard deviation
vol %	volume percent
wt %	weight percent

EVALUATION OF THE TIN-TUNGSTEN - GREISEN MINERALIZATION AND ASSOCIATED GRANITE AT SLEITAT MOUNTAIN, SOUTHWESTERN ALASKA

By Roger E. Burleigh[1]

ABSTRACT

In June, 1989, the U.S. Bureau of Mines, undertook a 9-day evaluation of the tin resource potential of the Sleitat Mountain tin deposit. Significant tin-tungsten mineralization is associated with quartz-topaz-white mica-tourmaline greisen alteration of a multi-unit, 57 Ma, peraluminous, granite stock which intrudes Cretaceous Kuskokwim Group flysch deposits. The granite comprises marginal biotite-, intermediate biotite-muscovite-, and central zinnwaldite-granite units, interpreted as a zoned alteration system. Major vein mineralization is confined to two east-west-trending zones of steeply oriented tabular lenses of greisen interleaved with mildly altered granite. Cassiterite is the dominant ore mineral while arsenopyrite, loellingite, wolframite, pyrite, sphalerite, chalcopyrite, and bismuth-oxides are present in minor to trace amounts.

The north and south greisen zones are estimated to contain an inferred resource of 128 to 212 million lbs Sn in 28.6 million st of mineralized rock. An 1,800-lb representative bulk sample contained 0.37% Sn, 0.04% W and 17 ppm Ag and is considered an average grade estimate for the deposit. Drill testing by Cominco Alaska Exploration indicates that substantial widths of high-grade tin mineralization are included within the lower grade disseminated mineralization. Depth of deposit erosion is substantial and there exists a high probability for placer tin deposits.

[1]Geologist, U.S. Bureau of Mines, Alaska Field Operations Center (AFOC), Fairbanks, Ak.

INTRODUCTION

Tin and tungsten are critical and strategic minerals to the United States. The basis for such a designation exists in the historic and current (1989) net import reliance of these metals by the United States as a percent of apparent consumption. Estimates by the U.S. Bureau of Mines for 1989 indicate a 73% net import reliance for both tin and tungsten (1)[2] with the balance derived largely from recycled scrap. Net import reliance is defined as imports minus exports plus adjustments for government and industry stock changes (1).

The identification of tin resources in the United States is critical due to the minimal tin reserves compared to the net import reliance. Most domestic tin resource potential lies in Alaska. Published estimates by Warner in 1985 (2) of tin resources in Alaskan lode and placer deposits are 96.0 million lbs of measured plus indicated and 44.9 million lbs inferred. By comparison, the United States consumed an apparent 107.6 million lbs of tin in 1989 (1).

The Sleitat Mountain tin-tungsten-silver deposit adds significantly to the tin resource base of the United States. This deposit was discovered, explored, and is owned by Cominco Alaska Exploration and an undisclosed joint venture partner. Cominco Alaska Exploration, at the request of the U.S. Bureau of Mines, allowed the Bureau to evaluate the deposit in 1989. The Bureau's evaluation included the following:

- ★ Geologic mapping of the deposit and surrounding rocks
- ★ Petrographic examination of mineralization and associated intrusive igneous rocks
- ★ Major oxide and trace element characterization of the deposit-related intrusive rocks
- ★ K/Ar dating of mineralization
- ★ A baseline sieved soil sample study
- ★ A baseline pan concentrate survey
- ★ Magnetometer, VLF-EM and radiometric geophysical characterization of the deposit and granitic rocks
- ★ An inferred estimate of the tin, tungsten, and silver resources of the deposit
- ★ Collection of an 1,800-lb bulk sample for mineral beneficiation testing
- ★ Rubidium-strontium isotope studies

The results of the beneficiation testing by the Bureau's Salt Lake City Research Center (UT) will be published in a separate Bureau of Mines report.

---

[2]Underlined numbers in parentheses refer to the list of references at the end of this report.

ACKNOWLEDGMENTS

Appreciation is extended to Helen Farnstrom, Project Geologist, Cominco Alaska Exploration of Anchorage, Alaska, for the opportunity to visit and study the mineralization at their Sleitat Mountain site. Technical reviews by Helen Farnstrom, Jeff Foley, Physical Scientist, AFOC-Anchorage, and Dr. Rainer Newberry, Associate Professor of Geology, Univ. of Alaska-Fairbanks greatly improved the organization and interpretations presented in this report. Geophysical data collection and reduction of VLF-EM and magnetic surveys was performed by Patricia Moore, geophysicist and temporary Physical Scientist AFOC-Fairbanks(AK). Acknowledgment is due to Cathy Summers, Geologist, Denver Research Center (CO), and Jane Knoper, analyst, with the Bureau's Albany Research Center (OR), for providing mineralogical data.

GEOGRAPHIC LOCATION AND ACCESS

Sleitat Mountain is located approximately 84 mi northeast of Dillingham and 80 mi west-northwest of Iliamna, southwestern Alaska, (section 31, T1S, R45W, of the Seward Meridian) (fig. 1).

The highest area of an isolated, northeast trending and elongate set of hills is host to the tin deposit (fig. 2). This isolated mountain rises above a widespread glacial gravel outwash plain that is pock-marked by numerous kettle lakes. The gravel plain would permit the landing of a small, tundra-tire equipped fixed-wing aircraft near the south side of Sleitat Mountain; otherwise, the deposit can only be reached by air with a helicopter. The word Sleitat means whetstone in Eskimo, in possible reference to the hard, flinty character of hornfels metamorphosed rock which occurs there. Patchy tundra covers surficial deposits of rubble and talus at the higher elevations, whereas, tundra and intermittent dense alder growth cover the flanks of the hills and drainages. The area is wind-swept by prevailing winds from the south.

GEOLOGY

Surficial Geology

An important consideration for any tin lode deposit is the potential for tin placer deposits in nearby surficial alluvial deposits. To the north and south of the small range of hills that contains the tin deposit, active gulch and stream drainage features dissect alluvial glacial outwash gravel terraces that lap onto the flanks of Sleitat Mountain. The active streams

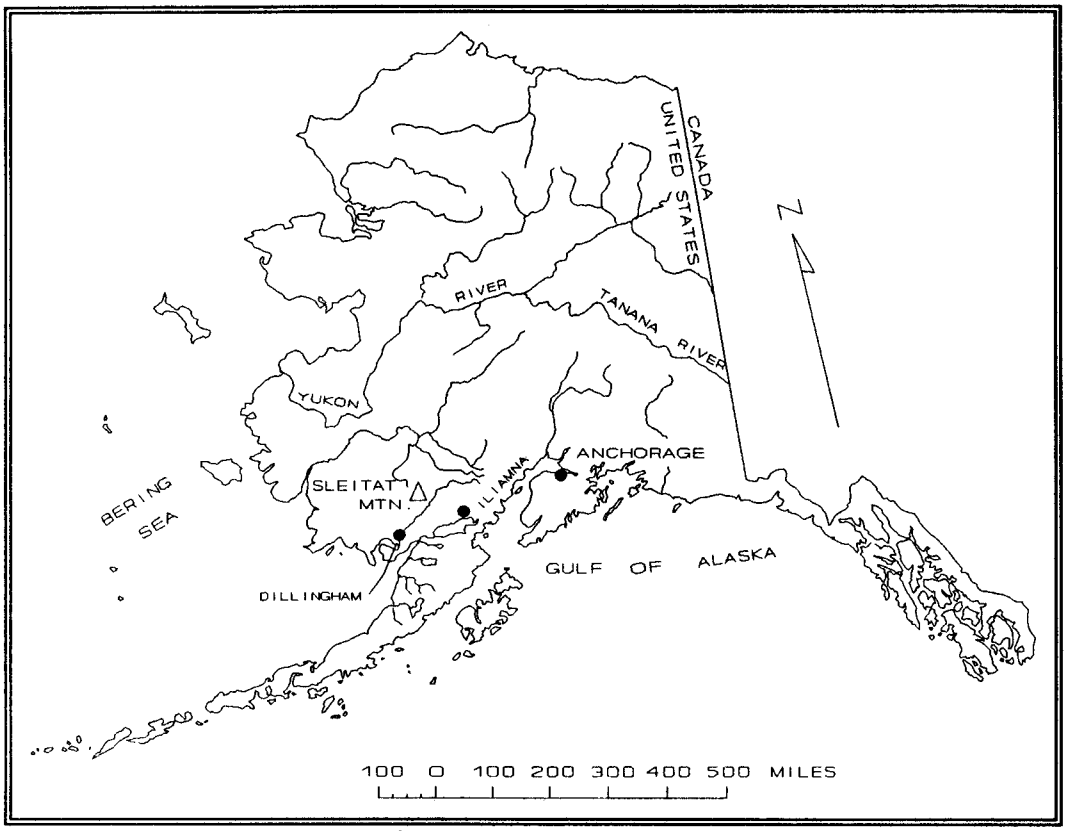

Figure 1. --Location map of the Sleitat Mountain tin deposit.

draining the deposit contain substantial amounts of cassiterite and wolframite. The terrace gravel contains volcanic rocks and chert pebbles that are not found in the local bedrock and does not contain anomalous concentrations of tin or tungsten.

Regional Geology

The recently discovered (1983) tin deposit at Sleitat Mountain is the only major tin prospect now known in southwestern Alaska. Elsewhere, tin deposits are usually found clustered in geologically permissive regions characterized by chemically distinctive, late stage, granite units related to differentiated batholithic or plutonic complexes (3). Although published geologic information on the region is not detailed, recent interpretations of the tectonic evolution of southwestern Alaska by Wallace and others (4) provide some basis for reconstructing the geology during and after the time of tin mineralization. The granite stock at Sleitat Mountain intrudes the Kuskokwim Group flysch deposits of late- Early Cretaceous to Late Cretaceous age

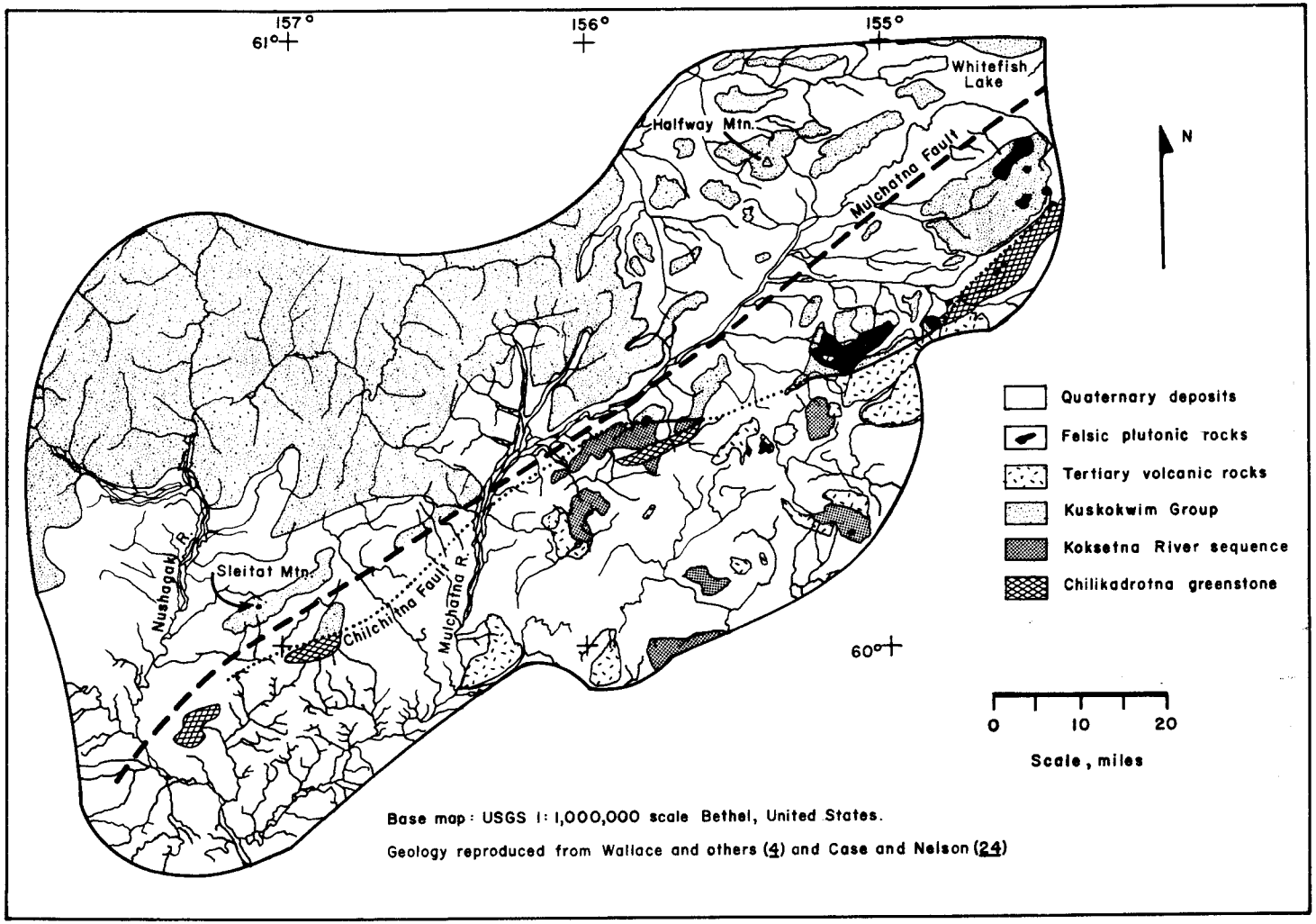

Figure 2. Regional geologic map.

(5). The Kuskokwim Group is a clastic sequence which depositionally overlaps many other terranes north and northwest of Sleitat Mountain. Sleitat Mountain lies within, but very near the south-southeastern border of exposed Kuskokwim Group rocks (fig. 2). Two major structural breaks occur along this southeastern border, the Chilchitna and Mulchatna Faults. Recent interpretations by Wallace and others (4), define the south-southeastern border of the Kuskokwim Group rocks as the Chilchitna Fault which separates the Kuskokwim Group from the older Kahiltna Terrane to the south. The Kahiltna Terrane comprises the Koksetna turbidite sequence of Late Jurassic to Early Cretaceous age and the Late Triassic to Early Jurassic age Chilikadrotna greeenstone (4). Wallace and others (4) mapped the contact between the Kuskokwim Group and the Kahiltna Terrane as sharp and steeply dipping to the northwest, placing the Kuskokwim Group over the Kahiltna Terrane. The juxtaposition of the Kuskokwim Group along the Chilchitna Fault was accompanied by a strong penetrative deformation which is suggested to have ceased by 71 Ma - the age of the oldest pluton in the region which post-dates the regional deformation as described by Wallace and others (4). These relations (see below) indicate that the structural juxtaposition of these rock units occurred approximately 11-16 Ma prior to mineralization at Sleitat Mountain.

Wallace and Engebretson (6) described four major Late Cretaceous to Paleocene magmatic belts in southwestern Alaska, and two of these belts, the Kuskokwim Mountains belt (73-60 Ma) and the Alaska Range belt (74-55 Ma), form parallel northeast-trending belts that are situated outboard of a central region of magmatic quiescence (fig. 3). In interior and southwestern Alaska, the Kuskokwim Group rocks, and the collective terranes which are overlapped by the Kuskokwim Group, are overprinted by these two magmatic belts.

The Sleitat Mountain granite occurs in the central region of magmatic quiescence. A single K/Ar determination[3] yielded an age of 56.8 ± 2.8 Ma for a coarse-grained muscovite mineral separate from a 0.3-in-thick muscovite veinlet. The muscovite formed during a late stage magmatic-hydrothermal event related to mineralization. It is unclear whether the Sleitat granite belongs to the Alaska Range or the Kuskokwim Mountains belt, or even if a magmatic continuum exists between these two belts. Wallace and Engebretson (6) have shown, however, that the Kuskokwim Mountains and Alaska Range belts have slightly different ages; the former belt has a mode of 70 Ma (range 73-60) and the latter a mode of 56 Ma (range 74-55). Hence, in terms of age relations, the Sleitat Mountain granite is more closely allied with the Alaska Range belt.

The granite stock at Sleitat Mountain is essentially elliptical in surface expression, has a thermal aureole, and

---

[3]Analysis by Teledyne Isotopes Laboratories, Westwood, New Jersey and the use of this lab does not imply endorsement by the U.S. Bureau of Mines.

associated volcanic rocks, if formerly present, do not outcrop in the immediate vicinity of the stock. Dikes which appear to extend from the stock, trend NE, parallel to the Mulchatna Fault.

Local Geology

Sleitat Mountain and the elongate set of hills extending in an east-northeast direction from its highest point are preserved due to a resistant hornfels aureole surrounding a small (< 1 mi^2)

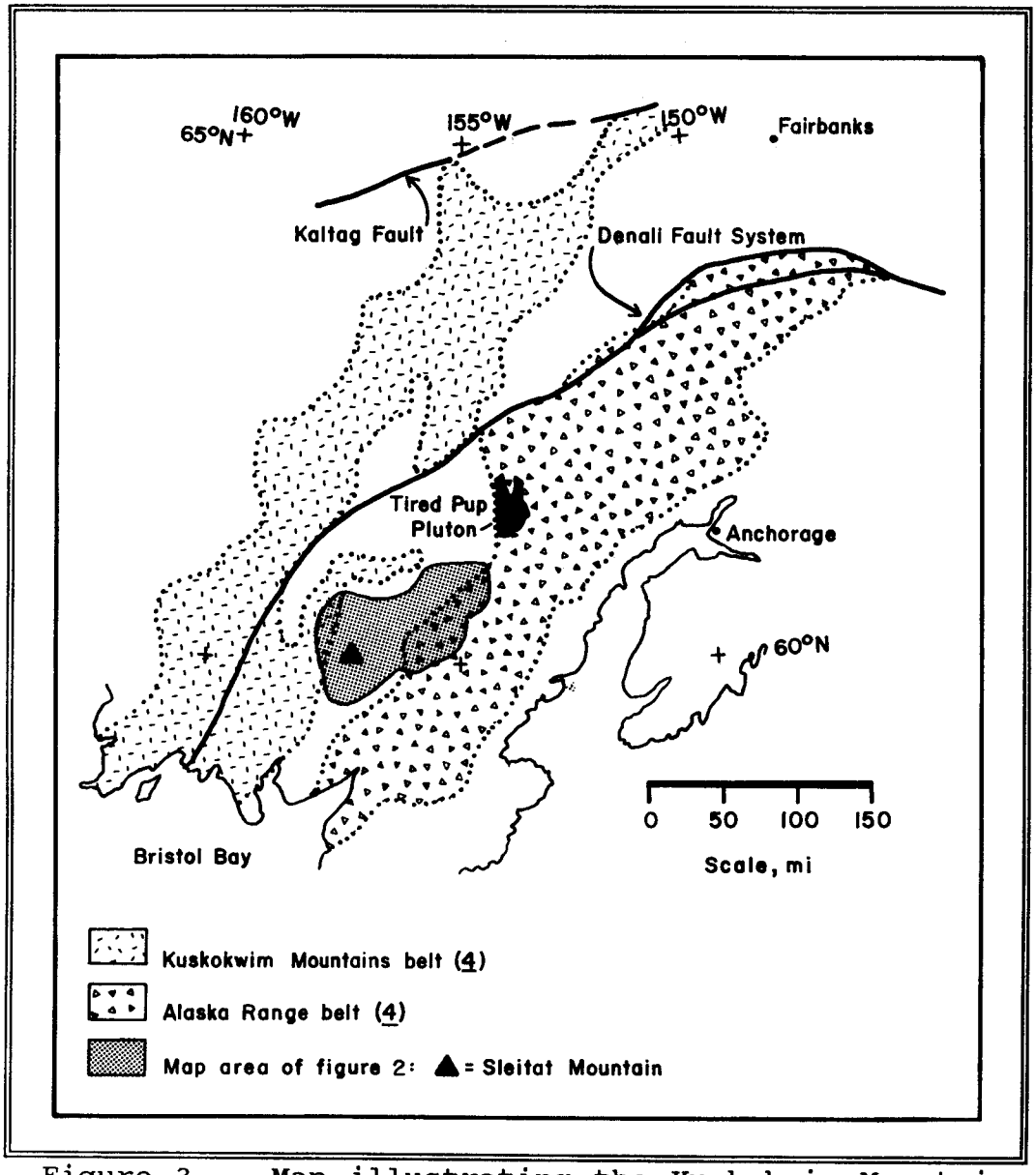

Figure 3. --Map illustrating the Kuskokwim Mountains and Alaska Range magmatic belts.

granite stock (fig. 4). The granite stock comprises biotite granite, biotite-muscovite granite, a zinnwaldite granite and extensive greisen alteration that overprints these three intrusive phases. At least two types of felsic dike rock occur on all sides of the stock. Contact relations of the dikes to the stock were not found exposed so the relative timing of their emplacement is unknown. The extent of hornfels development was not mapped in detail, however, thermal metamorphic affects generally extend 1,500 to 2,000 ft from the edge of the stock in all directions.

Igneous Petrology

Igneous rocks which comprise the Sleitat granite stock may be distinguished on the basis of mineralogical and petrological criteria, and are further shown to exhibit systematic geochemical variations between the three units. The granite units are mapped according to spatial distribution of relatively in-situ rubble-crop, as, nowhere does the granite form outcrop (fig. 4). It was not possible to map the distibution of biotite granite, as only local concentrations of rocks from this unit were present in the rubble-crop. These concentrations were present near the margin of the stock. The zinnwaldite granite unit appears to form the core of the stock with apophyses of this unit extending into the biotite-muscovite granite. This apparant physical relationship coupled with petrographic and geochemical evidence discussed below, either suggests that the zinnwaldite granite unit is the latest igneous unit to crystallize, or else an alteration event is superimposed on the stock that decreases in intensity from the center to the margin.

Biotite Granite

The biotite granite consists of hypidiomorphic, fine- to medium-sized grains of quartz, alkali-feldspar (perthite), plagioclase, biotite, topaz, and garnet with a seriate to weakly porphyritic texture. The perthite and quartz exhibit bimodal grain sizes with the size difference less than 10 times. The other minerals are fine-grained and are generally anhedral. Examples of rock textures for the biotite granite and other igneous units are presented in figure 5.

Quartz is present as 1-5 mm diameter grain aggregates, with some aggregates having square outlines suggesting beta-quartz, and as anhedral grains 0.5 mm or less in diameter. Perthite, forms sub-hedral, rectangular grains to 3-7 mm in size and finer grained aggregates with anhedral grains less than 2 mm across. The perthite contains approximately 35-45% exsolved albite lamellae. Anhedral plagioclase (5 to 10 %) is albite in composition based on petrographic determinations. Biotite is green to red-brown in color, forming sub-hedral to anhedral

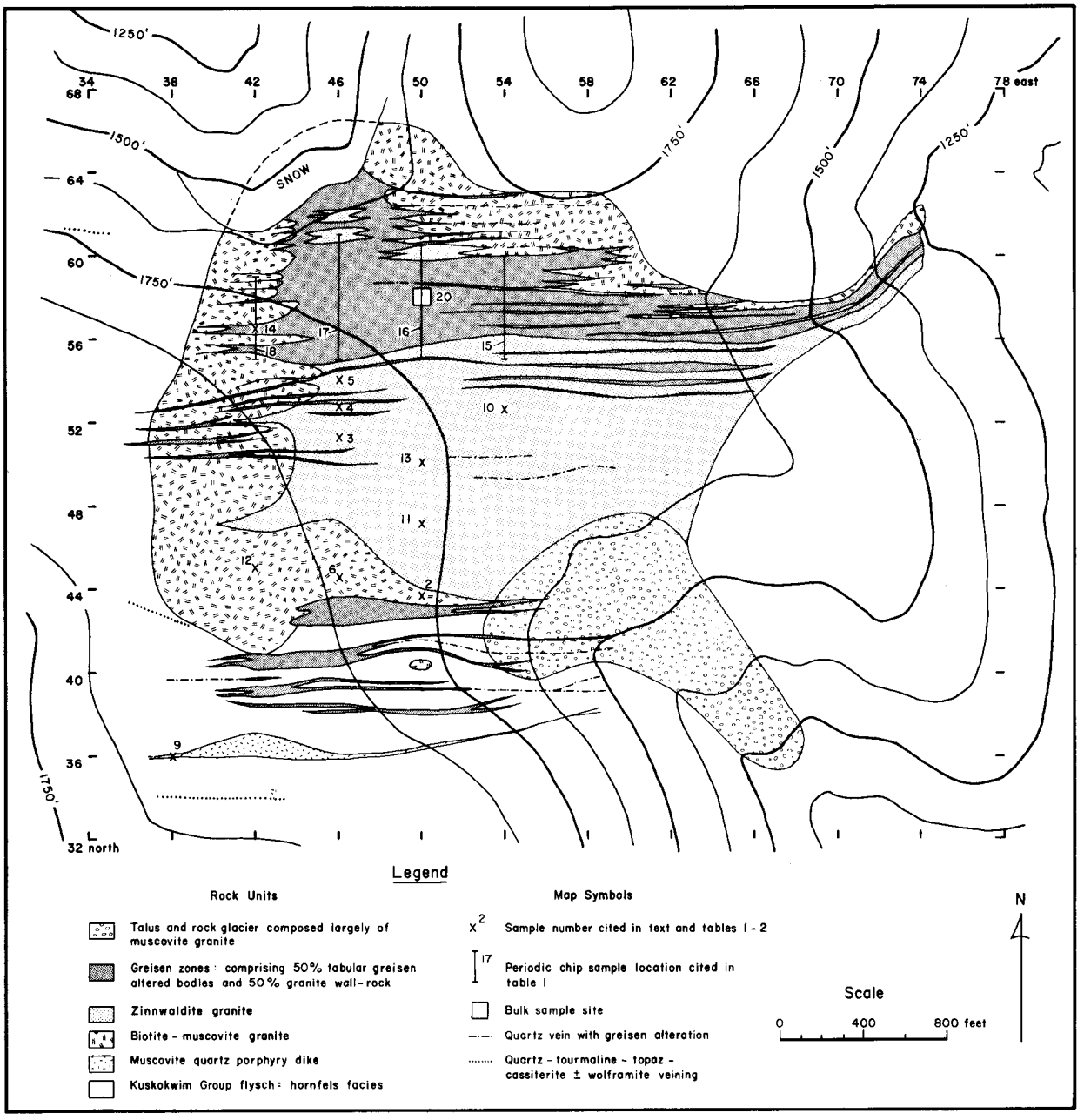

Figure 4. --Local geologic map and sample locations.

disseminated grains. All of the biotite contains minor amounts of accessory minerals, some of which impart metamict haloes in the biotite. Topaz is present as disseminated anhedral and rare euhedral grains that are preferentially associated with the fine-grained interstitial quartz and not the square-shaped quartz. Because the topaz is included within the coarser grains of interstitial quartz it appears to be a primary magmatic unit. Topaz accounts for less than 1% of the rock-forming minerals. Garnet occurs as disseminated anhedral grains that form much less than 0.5% of the rock. Accessory minerals (tentatively identified as zircon and monazite) are largely associated with biotite and less commonly are found associated with the quartz and feldspar minerals.

Alteration in the biotite granite is weak, and consists of feldspars, 10-20 % altered to sericite, and red-brown "book" biotite 0-5% altered to fine-grained green biotite.

Biotite-Muscovite Granite

The biotite-muscovite granite is generally fine- to medium-grained (up to 10 mm), weakly seriate to equigranular textured, and contains varied trace amounts of topaz, garnet, and tourmaline (fig. 5). Crystal size varies with mineralogy. Alkali feldspar (perthite) is present as medium (up to 10 mm) subhedral, tabular grains and smaller (0.5 - 5 mm) anhedral grains that both contain abundant patches and veins of albite.

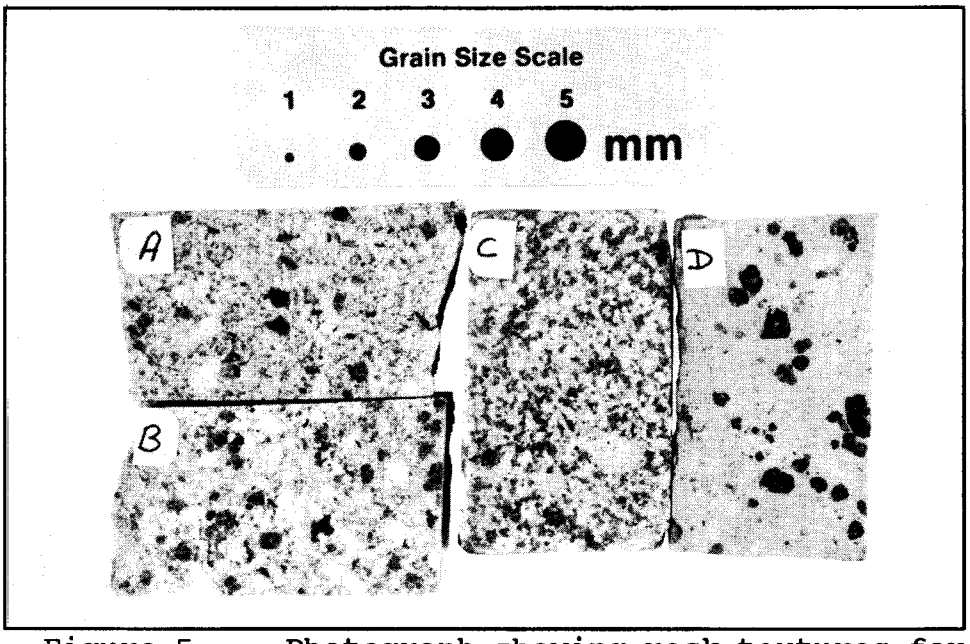

Figure 5. --Photograph showing rock textures for (A) biotite granite, (B) biotite-muscovite granite, (C) zinnwaldite granite, (D) feldspar-porphyry dike.

Exsolved albite accounts for approximately 20 to 45 vol % of the alkali feldspar. Alkali feldspar grains also contain small grains of plagioclase and small (<0.5 mm) rounded quartz inclusions that often are distributed in concentric zones. Albite (10 to 20 %) occurs as 0.1- to 3-mm anhedral grains that are often zoned and some have turbid cores. Quartz is present as <0.1-mm to 10-mm anhedral grains. Large quartz grains have undulatory extinction and interlocking grain boundaries with feldspars. Very fine-grained quartz (<0.1 mm) has normal extinction and is abundant in a semi-continuous network of rounded interstitial grains resembling bird shot. Fine-grained (0.1-3 mm) biotite is light red-brown (mostly) to dark red-brown in color with metamict accessory mineral inclusions. Biotite is subhedral to anhedral and typically is altered to muscovite along grain edges and/or surrounded and embayed by coarse-grained white mica. The light red-brown "bleached" biotite and secondary muscovite commonly contain trains of rutile indicating titanium mobilization during biotite alteration. Fine-grained (0.1-3-mm) muscovite, or white mica, is present as both ragged and angular-shaped interstitial grains and as felty masses. Muscovite also surrounds and embays angular feldspar grains suggesting a replacement origin for some muscovite. In places, muscovite contains fine-grained garnet or rare accessory minerals and is usually associated with very light-blue topaz and tourmaline. Disseminated subhedral to anhedral topaz and muscovite are also loosely distributed in vein-like patterns associated with other interstitial minerals. Rare, light-blue, blue-green to red-brown tourmaline occurs along cleavage traces in alkali feldspar and is spatially associated with particularly ragged-textured interstitial minerals. Interstitial minerals are markedly finer-grained, anhedral and include topaz, tourmaline, and muscovite that are intimately associated with abundant very fine-grained quartz.

Zinnwaldite Granite

The zinnwaldite granite forms the core of the granite stock, (fig. 4). Overall, this unit is fine-grained but textures vary from distinctly hypidiomorphic equigranular to micro-scale xenomorphic seriate (fig. 5). Alkali feldspar is present as 2- to 4-mm, anhedral to subhedral tabular grains and 0.1- to 2-mm, anhedral grains. Exsolved patchy and veined albite accounts for 5-15 vol % of the alkali feldspar (perthite) grains, notably less than in the biotite-muscovite granites, however, individual albite grains account for 25 to 35 % of the rock. Small grains of quartz, plagioclase and alkali feldspar are included in the larger alkali feldspar crystals. In some samples, quartz is present as rounded aggregates of anhedral crystals 1 to 4 mm in diameter and as interstitial anhedral grains ranging from <0.1 to 2 mm in size. Light grey-brown, pleochroic to colorless, white-mica occurs as ragged anhedral grains ranging in size from <0.1

to 1 mm. An X-ray Photoelectron Spectroscopy (XPS) evaluation of the white-micas suggests zinnwaldite as the most feasible composition. XPS analysis determined that fluorine is a constituent of the white mica, however, the presence of lithium was deduced by subtracting the interference caused by iron peaks in the spectra. Zinnwaldite appears to replace, or form intimate intergrowths with quartz and alkali feldspar. Blue to blue-green tourmaline is present in concentrations that range from <<0.5 to 5 vol % of the zinnwaldite granite.

In the hypidiomorphic to near graphic textured fine-grained zinnwaldite granites, abundant and disseminated hydrous minerals including tourmaline and topaz, appear unaltered and subhedral. In contrast, the more seriate textured granites (bimodal quartz grain size) contain low concentrations of tourmaline, present as net-textured replacements in alkali feldspar. Here, topaz forms colorless grains up to 1 mm in size and is always spatially associated with zinnwaldite and tourmaline in a mineral assemblage that is generally interstitial to a coarser-grained aggregate of alkali feldspar, quartz, and plagioclase. Other variants of zinnwaldite granite in which the overall texture is seriate, and where the grain boundaries of alkali feldspar and plagioclase tend to be ragged and allotriomorphic, contain only minor amounts of anhedral tourmaline and topaz.

Dike rocks

Two types of dike-rock were observed at Sleitat Mountain. A third type, biotite quartz porphyry, was identified by Cominco Alaska Exploration but not observed or sampled during this investigation. Muscovite-quartz-feldspar porphyry (muscovite porphyry) and quartz-feldspar porphyry (feldspar porphyry) dikes (fig. 5) occur peripheral to the stock on all sides and trend east-northeast (fig. 6).

Muscovite porphyry dikes are composed of about 35-40 vol % 0.5-5-mm, anhedral to subhedral, alkali feldspar, quartz, muscovite, and lesser plagioclase (albite) in a groundmass of very fine-grained (<<0.1 mm) feldspar, quartz, and muscovite. Muscovite-tourmaline micro-veinlets cross-cut both the groundmass and the phenocrysts. Alteration minerals include irregular patches and disseminations of tourmaline and muscovite throughout the groundmass and in feldspars. Megascopic quartz generally exhibits undulatory extinctions. The feldspar porphyry dikes differ mineralogically and chemically from the muscovite porphyry dikes. The feldspar porphyry dikes lack the coarser-grained muscovite and tourmaline and the feldspar phenocrysts range from 0.1 to 8 mm and form subhedral to euhedral grains and glomeroporphyritic aggregates. The groundmass of the feldspar porphyry dikes is sprinkled with very fine-grained white mica and is finer-grained, by an order of magnitude, than the muscovite porphyry dikes. Tourmaline is notably absent in the feldspar porphyry dikes.

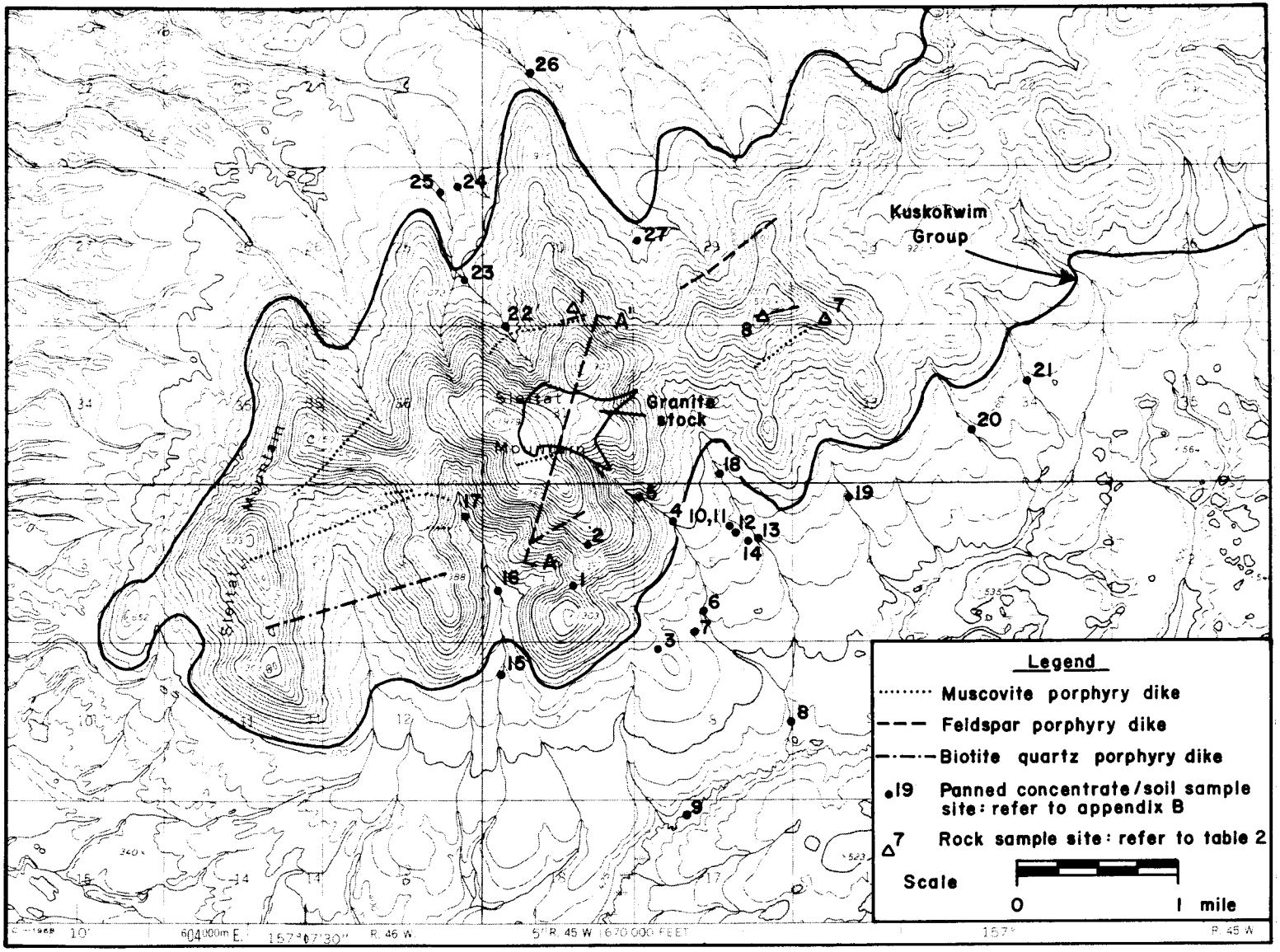

Figure 6. Geologic map of the Sleitat Mountain area with panned concentrate, soil, and rock sample locations.

The formation of coarse muscovite grains, vein and disseminated tourmaline, a coarsening of the groundmass, and turbid alteration of feldspar phenocrysts in the muscovite porphyry dikes indicate that the muscovite porphyry dikes are altered counterparts of the feldspar porphyry dikes. There is also a gross textural similarity between these dikes. Quartz-cassiterite mineralization was noted in an altered muscovite porphyry dike at grid location 51+00N, 36+25E (fig. 4).

Mineralization

Tin mineralization at Sleitat Mountain is expressed in all recognized units of granitic rock as well as the overlying hornfels. A diversity of gangue and ore mineral suites can be found in select samples of each rock type. In the greisen bodies that make up the bulk of the deposit, however, the observed quartz-topaz-tourmaline-white mica alteration assemblage exhibits little variation and is uniformly massive and granular. Furthermore, remnant quartz mineral textures in the greisen bodies reflect which granite unit underwent greisen alteration.

The principal ore minerals identified at Sleitat Mountain include cassiterite, arsenopyrite, loellingite, sphalerite, and wolframite. Trace amounts of stannite, chalcopyrite, pyrite, bismite, bismuth-arsenic compounds, and ferrotantalite were identified by scanning electron microscopy analysis (SEM) performed by the Bureau's Albany Research Center, Albany, Oregon. Secondary hematite and arsenic-oxides widely occur in weathered greisen samples.

Deposit Morphology

Cassiterite is present in a variety of vein and greisen structures. In the hornfels, coarse-grained quartz and quartz-topaz veins cross-cut sedimentary layers and fill partings along bedding in the meta-sedimentary rocks. These veins contain up to several percent fine- to coarse-grained black cassiterite and minor amounts of wolframite. Discordant veins up to 1.5 ft thick with strike lengths of a few hundred feet were observed in rubble-trains of vein material. Quartz veining that developed along partings was found only in scree accumulations so their continuity and widths could not be established.

Preliminary drill testing by Cominco Alaska Exploration indicates the bulk of the tin at Sleitat is found in steeply dipping tabular greisen bodies within the granite stock (H.E. Farnstrom, pers. comm.) (7). The greisen bodies are concentrated in two zones situated within the northern and southern margins of the stock (fig. 4). Individual greisen-altered bodies are vein-like and tabular in form. Central quartz veinlets, up to a few inches thick with local high concentrations (up to 50-60%) of fine- to coarse-grained cassiterite, appear to be the locus of

Figure 7. --Photograph of high-grade cassiterite-quartz vein and quartz-topaz-white mica-tourmaline greisen.

greisen alteration (fig. 7). The greisen alteration appears to extend normal to veining. Individual greisen bodies range from a few inches to 20 ft and are separated by mildly altered to unaltered granites. The zones of greisen mineralization comprise about 50% greisen-altered granite interleaved with essentially unaltered granite and extend for at least 3,200 ft with widths ranging between 100 to 800 ft (fig. 4). Greisen alteration also developed in association with wolframite-arsenopyrite veining, however, the dimensions and character of greisen alteration surrounding this vein type grades into, or can not be distinquished from, cassiterite-greisen in the rubble crop. Cassiterite is rarely observed in the presence of wolframite and if found together, euhedral cassiterite grains occupy open spaces within quartz-arsenopyrite-wolframite veins.

Alteration

Alteration mineral assemblages consist of variably increasing proportions of quartz, topaz, white mica, tourmaline, and clay minerals. Generally, however, the greisen alteration consists of major amounts of fine-grained quartz and topaz with lesser white mica and minor disseminated blue-green tourmaline. An extreme variation is represented by tourmaline-rich zones that appear to cut vein-like through the massive, granular, quartz-topaz greisen.

Clay-lined open-spaced voids are commonly disseminated in

the highly greisenized granite. Destruction and incomplete replacement of feldspar and phyllosilicate minerals by quartz, topaz, white mica and tourmaline, largely produced this porous texture. Most of the surface rubble exhibit iron, and to a lesser degree, arsenic oxide (scorodite) secondary minerals suggestive of approximately 1 to 5% original sulfide mineral content. With the leaching of these sulfide minerals, weathering has also contributed to increasing porosity of the greisen altered granite.

Ore Mineralogy

Cassiterite is the primary ore mineral at Sleitat. Grain size of disseminated cassiterite in the massive greisen-bodies is generally less than 1 mm. Medium- to coarse-grained cassiterite (1 mm to 1.5 cm) is found in high concentrations in narrow quartz veinlets within the greisen bodies and in the hornfels. Also, rare, open-space veinlets of coarse topaz with crystals of cassiterite and wolframite occur in hornfels peripheral to the greisen zones.

Wolframite occurs sporadically throughout the deposit, most notably as medium to coarse (up to 2 cm) tabular grains in massive to vuggy, coarse-grained quartz veins. These veins attain widths up to 2 ft and appear to represent a distinct mineralizing phase. Coarse grains of anhedral arsenopyrite are usually associated with the wolframite in these veins. Wolframite-rich vein specimens were generally found in the rubble peripheral to the greisen zones and within the hornfels. Fine-grained wolframite also occurs as a trace constituent in the tin-rich greisens.

Arsenic minerals are widely found throughout the deposit. Large clots of arsenopyrite (up to 1 inch) are common in coarse-grained, quartz-white mica-wolframite veins. Relatively unaltered and foliated biotite-muscovite granite specimens were locally found to contain ≈ 5% disseminated loellingite ($FeAs_2$) grains that have inclusions of bismite (bismuth oxide) and minute amounts of arsenopyrite. Generally, disseminated arsenopyrite is the primary As-mineral occurring at concentrations of up to 5% in greisen-altered granitic rocks in the absence of loellingite. Scanning electron microscopy (SEM) of arsenopyrite by the Bureau found micron-sized inclusions of bismite and a bismuth-arsenic mineral.

Sphalerite is rarely present in most greisen samples examined, however, a few specimens were found to contain up to 0.5 % disseminated sphalerite. Sphalerite contains micron-sized inclusions of bornite, chalcopyrite, and stannite. Coarser stannite grains (≈ 400μm) occur adjoined to grain boundaries of sphalerite, and as otherwise disseminated grains in the zinc-rich samples. A single, 30μm grain of ferrotantalite was observed in greisen-altered granite during SEM analysis.

TIN RESOURCE ESTIMATION

A principal goal of the Bureau's evaluation was to estimate the lode tin resource potential at Sleitat Mountain. Based upon the morphology of the deposit as determined by surface mapping and subsurface information provided by H.E. Farnstrom (pers. comm.) (7), a selective mining of the thick, near vertical, tabular greisen bodies by open pit methods is considered practical. The tabular greisen bodies are interleaved within otherwise barren granite, therefore a rubble-crop sampling method that determined both the ratio of granite to greisen in the greisen zones and the average tin grade of granite and greisen was applied.

The tin grade of greisen and granite and the density of greisen bodies was estimated by taking four, 400- to 600-ft-long, periodic chip samples across the northern greisen zone and partitioning the chips into one composite granite and one composite greisen sample per crossline (fig. 4). A chip was taken at each three-foot-interval, and if the interval station was on granite (or greisen) it was sampled and a count of the number of granite (or greisen) chips provided an assessment of the relative abundance of the two rock types. Analytical results from this sampling program are presented in table 1.

Table 1. --Analytical data for ore reserve estimation calculations

Crossline (feet)	Interval (feet)	Map* Number	Rock Type	Sn ppm	W ppm	Ag ppm	Nb ppm	Ta ppm	Greisen/Granite† Ratio
54+00E	55-60+00	15	Greisen	1900	150	16.7	23	<3	83/84
	North		Granite	120	45	0.7	26	<3	
50+00E	55-60+50	16	Greisen	2900	110	13.1	30	<3	82/69
	North		Granite	75	45	1.0	32	9	
46+00E	55-61+00	17	Greisen	3100	110	11.2	18	12	99/96
	North		Granite	930	45	2.5	26	<3	
42+00E	55-59+00	18	Greisen	880	150	7.0	33	<3	52/85
	North		Granite	2100	900	7.4	24	9	
								† Total	316/334

* Denotes a reference to the geologic map, figure 4.
† Number of sampled greisen intervals/number of granite intervals

The first three samples listed in table 1 represent the center of the northern greisen zone. These samples exhibit relatively uniform concentrations of tin, tungsten, and silver in the granite and greisen samples. The fourth sample listed in table 1, however, indicates the feathering out of the greisen veins at the western edge of the northern greisen zone. This is revealed by the lower greisen/granite ratio. In this western-

most sample site, thin (mm) cassiterite mineralized veinlets were observed in some of the granite chips collected, which accounts for the higher tin values as compared to the greisen sample. As a rule, the few obvious high-grade cassiterite veinlets encountered while sampling the massive greisen-altered rock were excluded from the sample chips to avoid nugget effects. Avoiding these veinlets probably contributes to an underestimation of the tin content of the greisen that occurs along all of the crosslines sampled.

By weighting the tin concentration of each crossline sample according to the number of 3-ft intervals in each greisen subsample (eg. 1,900 ppm X 83 greisen chips), an average tin concentration for the four greisen samples is obtained by dividing the sum of the weights by the total number of chips collected (316 chips). A value of 2,237 ppm Sn (.22 % Sn) is derived from this method. This value must be taken as the lower grade estimate for the deposit due to the sampling bias imposed to prevent nugget effects. The 1,800 lb bulk sample (no. 15, table 2) collected from the center of the northern greisen zone gave an assay of 3,700 ppm Sn (0.37 % Sn) which may be a more representative grade for the deposit. High grade zones can be expected at Sleitat Mountain and will substantially affect ore reserve estimates. One of Cominco's diamond drill holes intersected 47.7 ft (true width) of 1.56% Sn, including 5 ft (true width) of 12.6% Sn and 5.7 oz/st Ag (H.E. Farnstrom, pers. comm.) (7).

A provisional tonnage estimate is based upon four criteria: (1) surface area of the greisen zones as mapped, (2) a ratio of greisen/granite as derived from the composite number of chips in the four periodic chip samples (table 1), (3) a 500 ft depth projection, and (4) a tonnage factor of 12 ft^3/st. A surface area estimate of the greisen zones was determined using a ten squares/in. grid overlay on a 570 ft/in. scale map of figure 4. Four hundred eighty four (484) squares were counted to represent the greisen zones, which is equivalent to a surface area of 1,414,248 ft^2. By summing the collective number of greisen and granite chips an estimated ratio of 0.946 is calculated for the value of greisen/granite. A 500-ft depth projection is based upon a minimum 350-ft drill-indicated depth extension of the vertically oriented tin mineralization (H.E. Farnstrom, pers. comm.) (7). By multiplying the surface area by a 500 ft depth projection and dividing this quantity by the tonnage factor (12 ft^3/st), it is estimated that the greisen zones contain an estimated 58.9 million st of rock. Only about one half of this tonnage, however, is estimated to be mineralized greisen, or about 28.6 million st of greisen by applying the above greisen/granite ratio. Considering that overall tin grades probably range between a minimum of 2,237 ppm (4.47 lbs/st) and 3,700 ppm (7.4 lbs/st) it is estimated that the greisen zones contain between 128 and 212 million lbs of tin respectively. The drill intercept cited above indicates that considerably higher grade material is available, but at lower tonnages.

The potential for placer tin deposits buried below the terrace outwash gravels flanking Sleitat Mountain remains unevaluated. By considering a N-S profile through the center of the stock (fig. 8), a minimum of 250-500 ft of granite plus mineralized greisen zones has conceivably been eroded. By applying this model of the stock and the character of mineralization, the potential for appreciable placer tin deposits in buried channels surrounding Sleitat Mountain appears realistic.

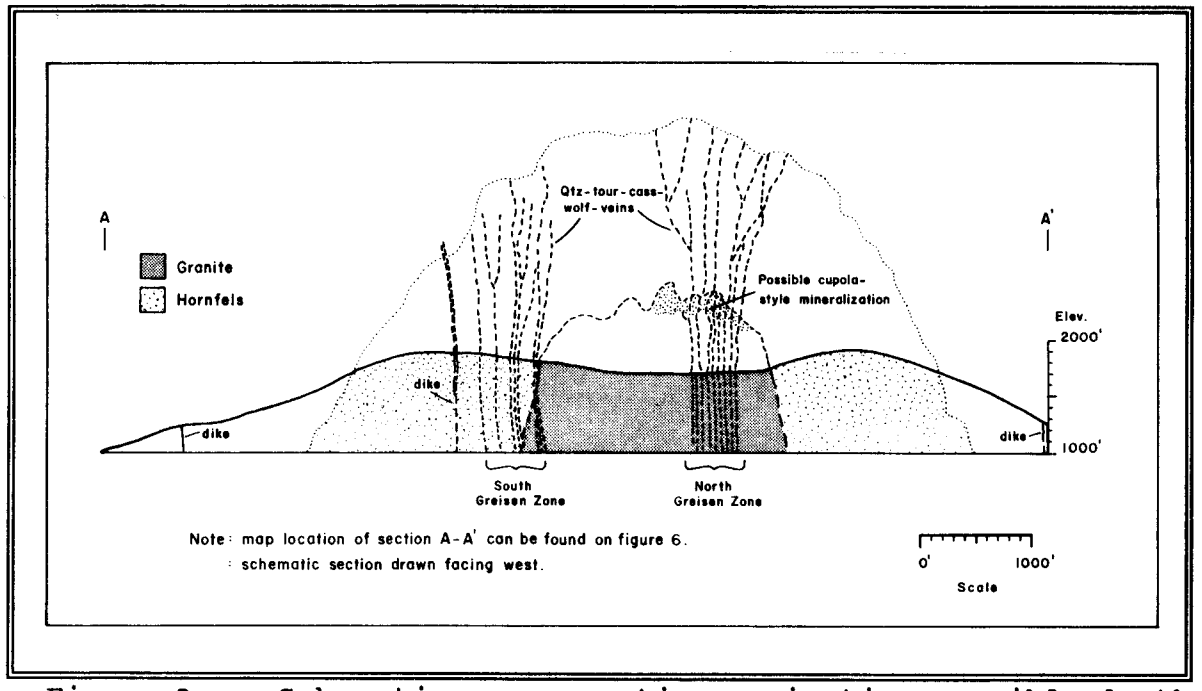

Figure 8. --Schematic cross-section projecting possible depth of erosion of the Sleitat stock and associated tin-greisen mineralization.

The trace elements niobium and tantalum are present in some tin-mineralized systems at concentrations sufficient to be important by-products of tin production. Although ferrotantalite was identified by SEM analysis, the few select samples (numbers 19, 20, 21, and 22, table 2, below) analyzed for niobium and tantalum did not contain significant concentrations of these elements. Furthermore, the chip samples collected for ore-reserve estimation purposes (table 1) were low in niobium and tantalum with concentrations comparable to the Sleitat Mountain granite, table 2.

EXPLORATION ASSESSMENT STUDIES

Geochemical studies of granitic rocks, overlying soils, and

nearby stream sediments, in conjunction with magnetometer, VLF-EM, and radiometric geophysical surveys were conducted on and around the Sleitat Mountain tin deposit. These investigations were conducted to evaluate methods of exploration that could be applied to undiscovered granite hosted tin deposits that might occur in the region.

Geochemistry of the Igneous Rocks

Granites related to tin deposits (tin-granites) are shown by several authors (Hudson and Arth (8) and Taylor (9)) to exhibit distinct geochemical characteristics which are perceived to be the products of extreme differentiation of a granitic magma. In many respects these geochemical characteristics also closely resemble compositions of 'topaz granite' described by Manning and Hill (10). Manning and Hill (10) propose that topaz-granite magma generation "may be controlled by limited partial melting of lower crustal fusion residues that had previously generated more 'normal' granite magma" and not the result of magmatic differentiation. Physical and temporal relations between the magmatic units at Sleitat Mountain cannot be adequately established due to lack of outcrop and exposed intrusive relations, however, a sequence of magmatic differentiation, and alteration history is indicated by the character and apparant systematic variation of major and trace element geochemistry between these units. Modelling the geochemical evolution of the Sleitat Mountain stock provides important criteria to the exploration geologist.

Major Elements

Systematic and incremental variations of major and trace elements, in a narrow range of composition, is evident between the three Sleitat Mountain granite units. Selected elemental data plots of:

1) K_2O/Na_2O vs. wt% SiO_2, 2) wt% TiO_2 vs. wt% CaO,

3) K_2O/Na_2O vs. wt% Al_2O_3, 4) Al_2O_3 vs. $CaO+Na_2O+K_2O$

(fig. 9a-9f), describe definable trends in major element compositions which can be interpreted as some combination of fractionation and progressive alteration. These plots show a systematic increase in Na_2O, Al_2O_3, and peraluminous index (molecular $Al_2O_3/Na_2O+CaO+K_2O$) with a concomitant decrease in SiO_2, K_2O, CaO, and TiO_2 from the marginal (biotite granite) to the core (zinnwaldite granite) intrusive units. The increase in Al_2O_3 is generally consistent with the progressive alteration of feldspars and biotite to white mica. Although depletion of CaO and TiO_2 is expected from increasing fractionation, the

alteration of plagioclase (Ca-depletion) and biotite (Ti-depletion) to white mica also provides a mechanism to produce these chemical trends. Major and trace element data are presented in table 2.

Table 2. --Major oxide and trace element analytical results for the igneous rocks

Map† Number	Sample Number	Al_2O_3 pct	CaO pct	Fe_2O_3 pct	FeO pct	K_2O pct	LOI pct	MgO pct	MnO pct	Na_2O pct	P_2O_5 pct	SiO_2 pct	TiO_2 pct	Totals pct
1	KS27153	14.30	.17	.44	.13	3.90	1.41	.07	.02	3.40	.14	74.80	.02	98.80
2	KS27189	13.20	.23	.43	.83	4.93	.53	.05	.06	3.52	.10	75.30	.03	99.21
3	KS27190	13.90	.21	.18	.70	4.33	.68	.02	.06	4.48	<.01	73.80	<.01	98.36
4	KS27191	13.10	.33	.36	.83	4.68	.67	.05	.06	3.70	.15	74.40	.02	98.35
5	KS27192	13.80	.34	.37	.57	4.51	.72	.04	.07	3.92	.07	75.20	.01	99.62
6	KS27193	13.40	.33	.51	.76	5.59	.51	.04	.13	3.55	.17	74.80	<.01	99.79
7	KS27199	15.20	.27	.79	.57	2.15	1.45	.35	.05	4.85	.19	73.90	.12	99.89
8	KS27200	13.60	.13	.54	.19	4.77	1.13	.11	.01	3.70	.05	74.90	.03	99.16
9	KS27201	15.00	.34	.31	.26	4.37	1.04	.18	<.01	3.93	.10	74.00	.12	99.65
10	KS27202	14.00	.18	.35	.64	4.19	.60	.04	.05	4.09	.16	73.80	.01	98.11
11	KS27204	13.80	.19	.60	.45	4.31	.37	.02	.06	4.20	.18	73.90	<.01	98.08
12	KS27212	13.20	.47	.38	.76	4.75	.37	.05	.06	3.86	.17	75.20	.03	99.30
13	KS27213	14.40	.17	.62	.64	4.20	.48	.02	.09	4.38	.12	75.60	.01	100.73
14	KS27223	12.60	.55	.31	.64	5.03	.58	.06	.04	3.43	.10	74.80	.04	98.18

Map† Number	Sample Number	Ba ppm	Nb ppm	Rb ppm	Sr ppm	Zr ppm	Y ppm	Sn ppm	Ce ppm	Ga ppm	Ta ppm	Rock Type
1	KS27153	<20	23	305	9	43	8	37	<5	34	-	Feldspar porphyry dike
2	KS27189	<20	23	425	<5	47	43	91	40	57	-	Biotite-muscovite granite
3	KS27190	<20	22	460	<5	24	38	200	10	70	-	Zinnwaldite granite
4	KS27191	30	27	395	<5	46	51	25	27	39	-	Biotite-muscovite granite
5	KS27192	<20	25	279.4*	10.3*	39	37	29	20	34	-	Biotite-muscovite granite
6	KS27193	<20	18	295	<5	38	54	21	13	16	-	Biotite-muscovite granite
7	KS27199	230	23	150	160	53	13	25	15	25	-	Muscovite porphyry dike
8	KS27200	600	23	240	81	44	26	29	27	43	-	Feldspar porphyry dike
9	KS27201	160	18	230	30	39	20	19	16	59	-	Muscovite porphyry dike
10	KS27202	<20	21	505	<5	34	41	22	13	83	-	Zinnwaldite granite
11	KS27204	<20	21	465	<5	25	34	31	15	73	-	Zinnwaldite granite
12	KS27212	30	21	335	9*	41	54	34	33	45	-	Biotite-muscovite granite
13	KS27213	<20	28	594.6*	2.1*	30	38	18	29	56	-	Zinnwaldite granite
14	KS27223	150	22	205.0*	25.96*	58	45	15	29	12	-	Biotite granite
19	KS27203	-	-	13	-	-	-	16000	39	<10	3	38" chip; greisen vein
20	KS27154	<100	27	90	-	-	35	3700	16	11	8	Greisen bulk sample
21	KS27194	-	21	-	-	-	-	15	33	43	5	Bio-gar-loellingite granite
22	KS27169	-	<5	-	-	-	-	92300	<5	39	13	Quartz-cassiterite vein

Note: Ba, Nb, Rb, Sr, Zr, Y, Sn, Ce, Ga, Ta analyzed by X-ray flourescence except where noted. Whole-rock oxides analyzed by direct coupled plasma emission after $HF-HNO_3-HClO_4-HCl$ extraction except for FeO. FeO analyzed by titrametric methods. An asterisk (*) denotes analysis by isotope dilution.

† Map numbers are referenced to figure 4.
- Not analyzed

Hudson and Arth (8) concluded that a positive correlation between Na_2O and differentiation index (DI) (11) for the most differentiated rocks (fine-grained equigranular phases) of Seward Peninsula tin-granites represents an evolutionary trend of crystallization. The development of this "albite trend" was suggested to be evidence that vapor-phase saturation was involved

in the crystallization history (8). For the Sleitat Mountain granite, data plots of wt% Na_2O versus DI indicate a progressive increase in Na_2O from marginal to core units, but only a weakly defined "albite trend" with respect to DI (fig. 9a). Petrographic examination of the three units shows a progressive increase in the presence of albite, (5-10%)→(10-20%)→(25-35%), from marginal to core units to account for the Na_2O trend.

In terms of Al_2O_3, SiO_2, Na_2O, K_2O, and based upon data from Tischendorf (12), the Sleitat Mountain granite has geochemical

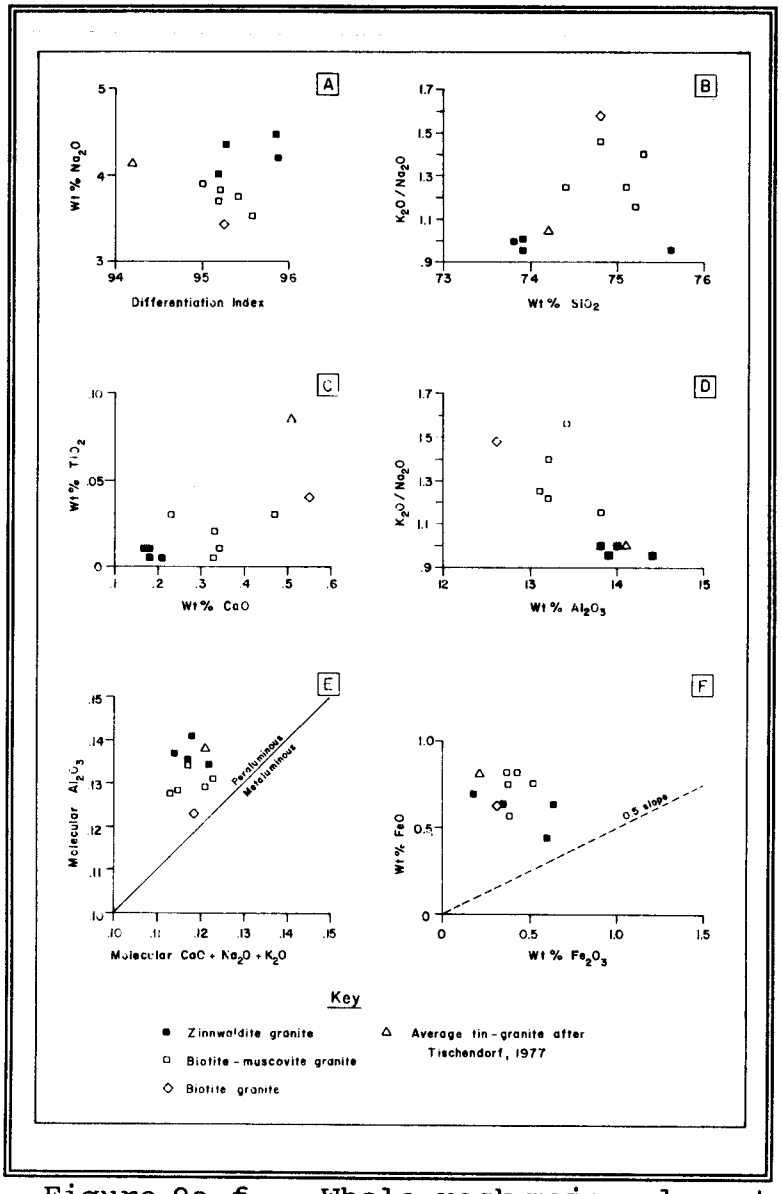

Figure 9a-f. --Whole-rock major element variation diagrams comparing the three granite units at Sleitat Mountain.

characteristics similar to the average tin-granite. Indices for an average tin-granite are included on figure 9a-f for reference. Plots of Na_2O vs. DI (fig. 9a) suggest that the Sleitat Mountain granite is slightly more fractionated than the average tin granite.

Trace Elements

Trace element analyses for lithium, fluorine, and boron were not obtained for Sleitat Mountain granites. Nevertheless, the respective increase in the amounts of tourmaline (B) and topaz (F) in the biotite-muscovite granite and the zinnwaldite granite units indicate increasing boron and fluorine content as noted in tin-granites elsewhere (10,12-13). The Sleitat Mountain samples show distribution patterns of decreasing barium and strontium and increasing rubidium (eg. samples 5, 13, 14, table 2) that are consistent with a highly fractionated granite as demonstrated by McCarthy and Hasty (14) and other tin-granites in the world (12). The variation characteristics for rubidium (fig. 10e), however, likely reflects an enrichment trend (Rb) and depletion trends (Ba, Sr) due to hydrothermal alteration of feldspars to white mica and albitization (15).

The elements zirconium, niobium, cerium, and yttrium, are generally useful indicators of magmatic trends because of their relative insensitivity to the effects of hydrothermal alteration (15). For the three granite types, however, individual data plots of gallium versus rubidium, zirconium, niobium and yttrium exhibit trends that can be interpreted to represent a singular melt fraction which had undergone systematic alteration from the core to the margins. Gallium remains mobile in a melt as a GaF_6^{-3} complex in fluorine-rich magmas (16). Gallium also tends to concentrate in plagioclase, substituting for aluminum, and is preferentially excluded from An-rich plagioclase (16). Hence, the gallium enrichment may be a function of topaz and albite formation in the core unit of the stock. Zirconium, and less so yttrium, exhibit depletion trends from core to marginal units. Alderton and others (15) observed strong depletions in zirconium concentration in similar granitic rocks as a result of tourmalinization and kaolinization and attributed the loss to the destruction of zircon during replacement of biotite by tourmaline. Hill and Manning (17) observed that inclusion free 'brown' mica (bleached biotite at Sleitat Mountain) in a topaz granite was derived from zircon-bearing biotite as a result of alteration. The enhanced degree of tourmalinization and the formation of bleached biotite and zinnwaldite in the core units of the Sleitat Mountain stock similarly suggests that zirconium depletion resulted from alteration and is not a function of melt fractionation (fig. 10a). Yttrium exhibits a similar, but weaker, depletion trend (fig. 10b) suggesting mobilization in response to hydrothermal alteration (tourmalinization). Niobium exhibits no enrichment or depletion trends in the granitic units

or greisen-altered rocks indicating immobility of this element to variable degrees of progressive greisen alteration (fig. 10c). The clustering of niobium values also suggests that magmatic fractionation played a limited role (if any) in forming the zoned granite stock. On average, a weak depletion trend for cerium occurs in the direction of biotite → biotite-muscovite → zinnwaldite granite units (fig. 10d). This trend generally parallels those of zirconium and yttrium. In the late-stage, equigranular fractions of Seward Peninsula tin-granites, Hudson and Arth (8), observed a cerium depletion and suggested that cerium is lost in conjunction with volatile-depletion of the latest crystallizing phases.

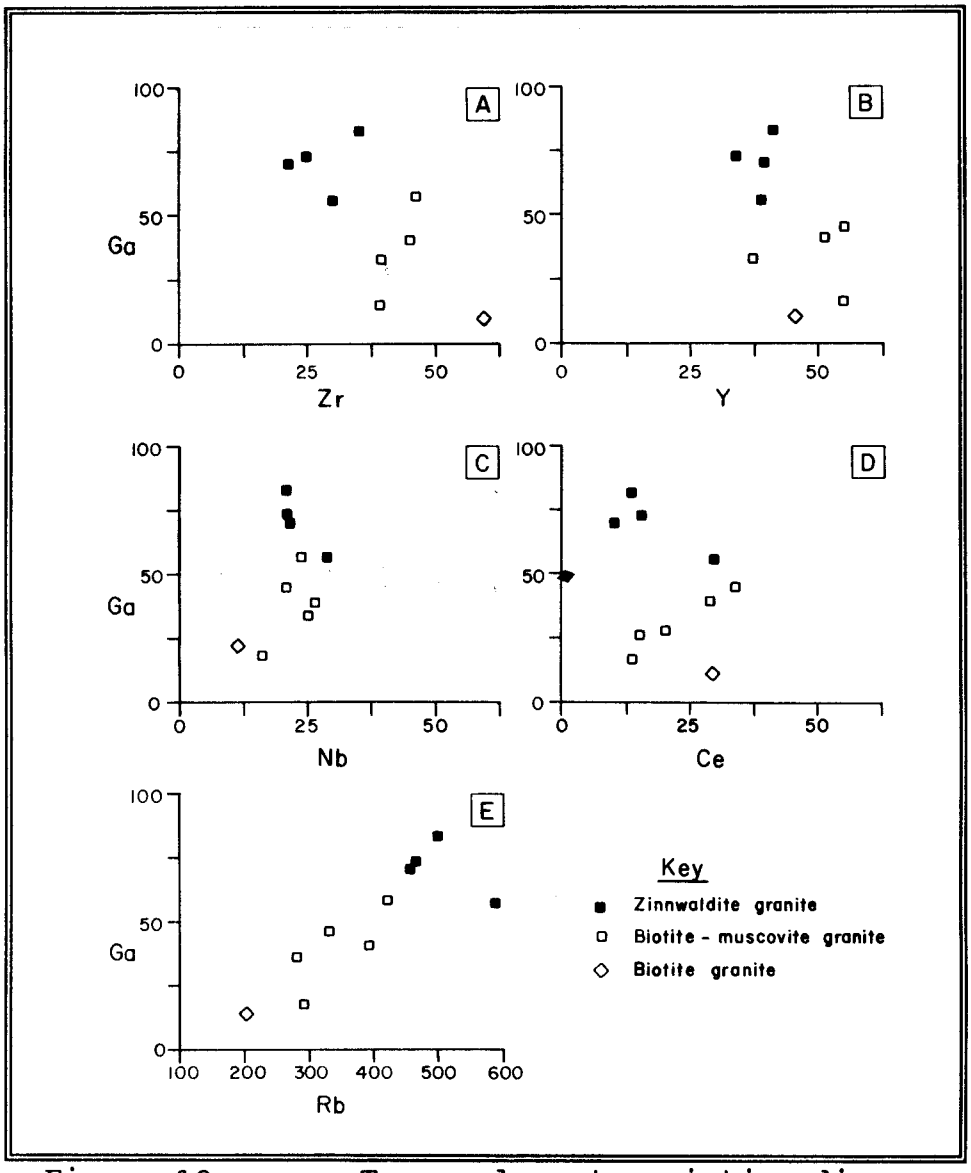

Figure 10a-e. --Trace-element variation diagrams comparing the three granite units at Sleitat Mountain.

Rubidium-Strontium Isotope Study

Strontium isotopic data and rubidium and strontium isotope dilution analyses for a sample of each of the three granitic units at Sleitat Mountain were obtained to determine initial $^{87}Sr/^{86}Sr$ ratios and to support the K-Ar age determination. A rubidium-strontium isochron calculated (method of Fauer and Powell (18)) for the three samples (table 3) yields an age of 44.1 Ma using the decay constant of $1.42X10^{-11}y^{-1}$ for ^{87}Rb. This age is discordant with the 56.8 Ma K-Ar age of vein muscovite discussed earlier. Rubidium-strontium ages calculated from pairs of samples yield ages of 45 Ma (samples 13 & 14), 79 ma (samples 14 & 5, and 610 Ma (samples 13 & 5; all of which are also discordant with the K-Ar age.

Table 3. --Rubidium-strontium isotope data and calculations

Sample†	$^{87}Sr/^{86}Sr$	$^{87}Rb/^{86}Sr$	$^{87}Sr/^{86}Sr_i$	Granite type
5	0.7861	78.9862	0.7224	Biotite-muscovite
13	1.2619	862.1279	0.5663	Zinnwaldite
14	0.7233	22.8535	0.7048	Biotite

†Sample numbers refer to analyses in table 2.

A calculation of the initial $^{87}Sr/^{86}Sr$ ratio ($^{87}Sr/^{86}Sr_i$) for each sample should yield nearly identical values if the magmatic rocks are cogenetic and unaltered. The calculated ratios are clearly discordant with one another, and in consideration of previous discussions on igneous petrology and geochemistry, it appears that these values reflect the effects of alteration. The least altered unit is the biotite granite, (sample 14, table 3), and the initial $^{87}Sr/^{86}Sr$ ratio of 0.7048 is the most reasonable initial value of the three samples. The $^{87}Sr/^{86}Sr_i$ of the biotite granite falls below the range of $^{87}Sr/^{86}Sr_i$ for the siliceous peraluminous Tired Pup granite (fig. 3) of the McKinley Sequence (0.7054-0.7085) (19) and the granitic rocks of the southwestern Kuskokwim Mountains (0.7060-0.7104) (20).

Discussion

The concentration of tin into late magmatic differentiates and magmatic fluids is suggested by Lehmann (21) to be due, in large part, to the oxidation state of the melt. Swanson and others (13) emphasize, however, that a given bulk composition of a melt which prevents the formation of tin-concentrating minerals such as sphene, hornblende, and Fe-Ti oxides, effectively results

in the retention of tin in the residual melt during fractional crystallization. They attribute the absence of hornblende and sphene to low concentrations of CaO and the absence of hornblende to a moderately peraluminous composition. It is essential though, that these conditions had prevailed in the less evolved granite fractions (ie. porphyritic and seriate fractions of Swanson and others (13)). At Sleitat Mountain, one can only surmise the presence of these fractions at depth as such granites are not exposed at the surface. There is no evidence, however, to indicate the existence of an associated plutonic complex and therefore other theories on the origin of 'topaz granites' like Sleitat Mountain merit consideration. Manning and Hill (10) propose a model in which lower crustal, refractory residues of previously generated biotite-granite magmas are partially melted to form a volatile-rich specialized magma that becomes emplaced in upper crustal rocks. This model removes the 'topaz granite' magma from generative processes of magmatic differentiation but still requires associative magmatic rocks. Conceivably, the Sleitat Mountain stock may have punctured an associated batholithic complex regardless of the model applied. For the exploration geologist, the example of the Sleitat Mountain tin deposit shows that significant tin mineralization is not always clearly associated with batholithic complexes.

Irrespective of the model applied to the Sleitat Mountain stock, the systematic variations in major and trace element geochemistry record the evolution of a magma, from which, late stage mineralizing fluids became fractionated. These hydrothermal fluids produced units of alteration that diminish from the core to the margins. Geochemical trends reflect the alteration pattern and provide useful exploration criteria for the discovery of similar mineralized systems in the region.

Heinrich (22) reviewed geologic evidence and tested quantitatively the chemistry of hydrothermal tin-tungsten transport and deposition processes and concluded that evolving, acid, magmatic fluids transport the bulk of the tin to sites of ore deposition and that these fluids evolve from the final melt fraction. At Sleitat Mountain, the major and trace element trends suggest that alteration of the Sleitat Mountain stock was approximately accompanied by greisen vein formation. It is essential to recognize that mineralization and alteration of the Sleitat Mountain stock resulted in the formation of thick, vertically oriented, tabular greisen-bodies with quartz-cassiterite veinlets and that magmatic-hydrothermal fluids must have circulated upwards along the east-west vein system from deeper levels of the igneous complex.

The thick (up to several feet) greisen altered margins of the quartz-cassiterite veins at Sleitat Mountain are mineralized with disseminated cassiterite in apparant response to acid-reducing alteration reactions (eg. feldspar to mica) (22). In lieu of acid-buffered reactions, however, the high-grade cassiterite-quartz feeder veinlets within the tabular greisen bodies probably formed in response to cooling fluid temperatures

as proposed by Heinrich (22). The cassiterite-rich quartz veins within the hornfels (no. 19, fig. 4), however, exhibit little alteration, and cooling fluid temperatures are probably responsible for cassiterite deposition here.

Field relations at Sleitat Mountain suggest that the quartz-wolframite-arsenopyrite vein system represents a separate mineralizing pulse, however, physiochemical differences in transport and deposition processes for tin and tungsten in hydrothermal fluids (22) may account for the apparent occurrence of separate mineralizing pulses at Sleitat Mountain. Heinrich (22) states that wolframite deposition is largely a function of fluid cooling, with or without fluid - wall-rock interaction. The wolframite-bearing veins observed at Sleitat Mountain are appreciably larger than the cassiterite-rich veins, and this larger size difference may have permitted more effective confined fluid flow and less wall-rock interaction, preventing acidity-reduction and significant cassiterite deposition.

Geophysical Surveys

Ground-based VLF-EM (Very Low Frequency Electromagnetics), total field magnetometer, and radiometric geophysical surveys were conducted over the Sleitat Mountain stock in order to rate their respective ability to delineate this style of mineralization. All three surveys were conducted along north-south crosslines which are normal to the trend of mineralization. The crosslines were spaced 400 feet apart and extended into the surrounding hornfels (fig. 4). Contour maps were produced to illustrate the results of the three surveys.

Magnetic Survey

The magnetic survey was conducted using a UNI-MAG II[4] proton magnetometer with the operator facing north at every station. Observations of the diurnal drift were made at intervals of less than two hours during the course of daily surveys. Subsequent to these observations, a diurnal drift correction was made in the construction of the contoured magnetic map (fig. 11).

The magnetic survey does not sucessfully define the large zones of greisen alteration mapped in figure 4. Two features are evident, however, from the contoured magnetic data. The first is the rapid decrease in magnetic susceptability outside and away from the stock contact in all directions, and the other is the broad magnetic high (400 gamma contour) that is off-centered and focussed over the south greisen zone. The dislocation of the

[4]UNI-MAG II is a trade name of EG&G Geometrics, 395 Java Drive, Sunnyvale, CA 94086 and its use does not constitute an endorsement by the U.S. Bureau of Mines.

magnetic high towards the south side of the relatively circular stock can be interpreted to represent a normal north-side-low effect for N-S profiles across a vertical cylindrical body (granite stock = the dipole); this a geologically reasonable configuration for the granite stock. The displacement of high magnetic contours toward the south side of a vertical cylindrical dipole is a consequence of the steep inclination of the earth's magnetic field at high latitudes (23).

The magnetic signatures expressed by the stock at Sleitat Mountain should be useful as a guide in regional exploration.

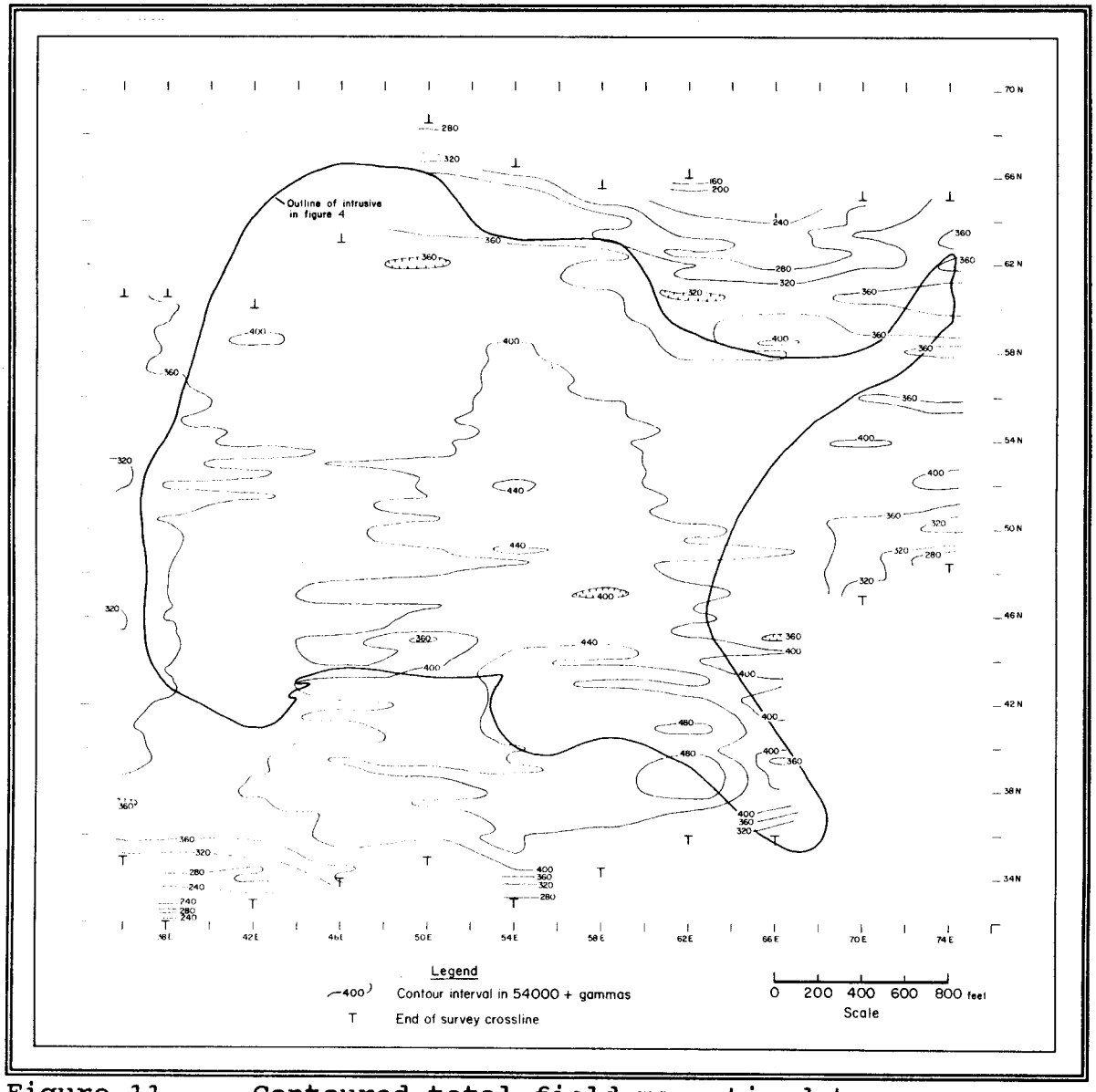

Figure 11. --Contoured total field magnetic data.

VLF-EM Survey

The VLF-EM survey was conducted using an EM-16 model instrument[5] with the operator facing northwest at every station. Station spacing was 100 ft apart along crosslines 400 ft apart. A normal procedure would utilize 50-ft-spacings along crosslines.

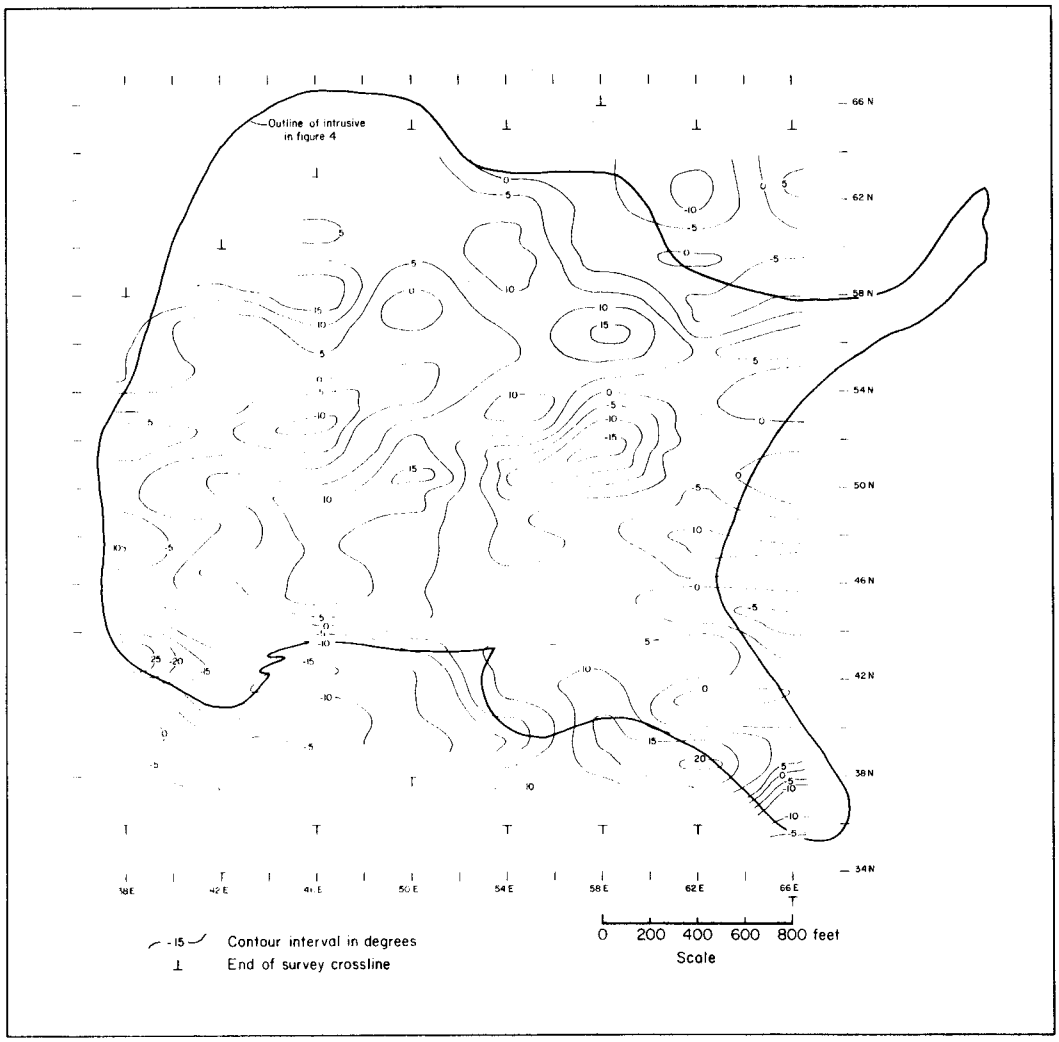

Figure 12. --Contoured Fraser-filtered, inphase component VLF-EM data.

[5]EM-16 is a trade name of GEONICS LTD. of Toronto, Canada and its use does not constitute an endorsement by the U.S. Bureau of Mines.

Time and weather constraints, coupled with an anticipated large target size (north and south greisen zones), affected the decision to apply a 100-ft-station spacing.

The VLF-EM survey method utilizes signals from VLF transmitting stations located around the world. In Alaska, stations located in Japan (NDT), Hawaii (NPM) and Seattle (NLK) generally provide signals of adequate strength. During the course of this survey Seattle and Japan signals were either too faint, or off due to maintenance. Only the Hawaii station could be used. The optimal configuration is to have the orientation of the potential conductor parallel to the direction of wave propagation from the VLF-station. The tabular greisen bodies are oriented at nearly right angles to the direction of Hawaii providing the least desirable configuration. The in-phase component of the data collected was reduced using a filtering procedure (24) and the filtered data was plotted and contoured (fig. 12). Positive contour intervals represent relatively conductive areas and negative contours are resistive.

Mapping has shown the greisen zones to be concentrated in elongate east-west oriented zones, however, the results from the Hawaii station do not show a particular resistive or conductive signature correlating with these mineralized structures. The VLF-EM geophysical method as applied to the greisen systems at Sleitat Mountain is inconclusive without using a more optimally aligned transmitting station such as Japan (NDT).

Radiometric Survey

The radiometric survey was conducted at the same time as the magnetometer survey by a separate operator stationed 50 ft away. A Scintrex GIS-Gamma Ray Spectrometer[6] instrument was used and readings were taken with a 10-sec integration time at 50-ft spacings along 400-ft crosslines. The radiometric survey was useful in defining several geologic features of the stock and mineralization. Figure 13 is a contour map of the raw data with an outline of the stock for reference. It clearly shows that radiometric readings drop off to the 100 gamma background range moving from the intrusive into the hornfels. The northern greisen zone appears to have a slightly weaker radiometric signature than the area of unaltered granite to the south. The unaltered granite appears to be generally outlined by the 180 gamma contour whereas coincident with the northern greisen zone there are large elongate areas of 140-180 gamma emmissions suggesting a depletion of radioactive elements in the greisens. This elongate area is punctuated by isolated high radiometric readings which probably reflect the interleaving of the tabular

[6]Scintrex GIS-Gamma Ray Spectrometer is a trade name of Scintrex of Canada and its use does not imply endorsement by the U.S. Bureau of Mines.

greisen zones with weakly altered granite.

At the eastern half of the south greisen zone radiometric readings are similar to those found in the northern greisen zone. This area is largely composed of hornfels rubble and appreciable amounts of granite or greisen rubble were not observed. These radiometric observations suggest that granite and/or greisen altered granite underlie the eastern half of the south greisen zone to a greater extent than mapped. In general, the radiometric survey has some value for distinquishing tin-greisen mineralization against a background of granitic host rocks. It also appears useful in mapping dike swarms (greisen veins of the south zone) against a background of hornfels country rock.

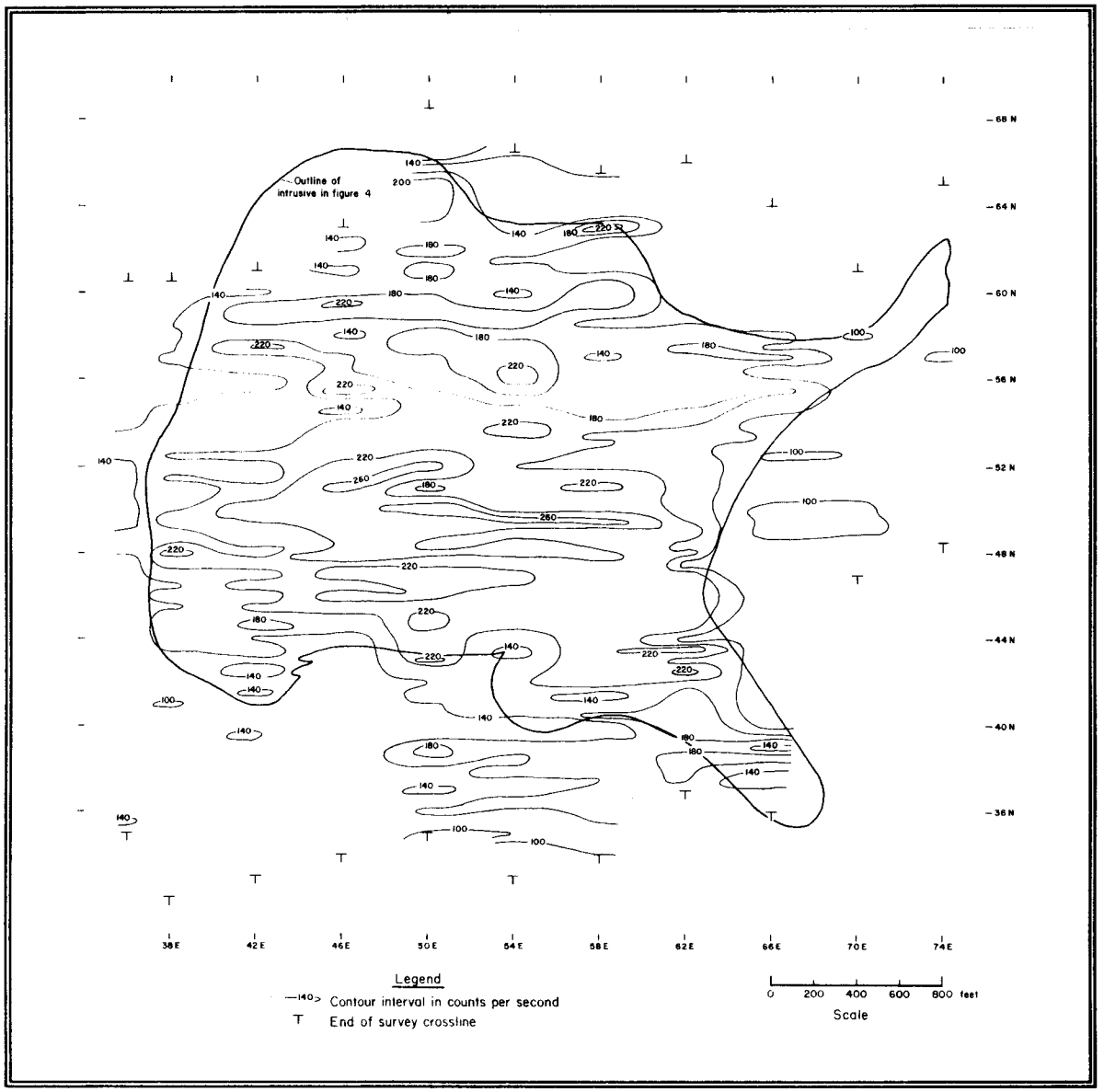

Figure 13. --Contoured radiometric data.

Soil Geochemical Survey

A baseline soil geochemical survey of tin, tungsten, and silver extending across the mineralized zones within the granite and into the overlying hornfels was undertaken to ascertain an optimal method of sampling a primary tin deposit. Crossline 42+00E (fig. 4) was chosen for the survey because it spanned an area of reasonably well-developed soil formation in contrast to the rubble deposits that cover most of the deposit. Along the profile, well developed frost polygon structures and frost boils occur in the soils on areas of flat terrain and thin, poorly formed rocky soil of sandy clay occur on steeper slopes. Sampling depth was 6 to 8 in.

All soil samples were wet-sieved into four size fractions of -80-, -28+80-, -14+28-, and +14-mesh material. The +14-mesh material was discarded. Bar graphs representing the concentrations of the three elements and a geologic cross-section along the profile are presented in figure 14. Analytical results are listed in appendix A. The bar graphs for tin and tungsten indicate that tin and tungsten are concentrated in the coarser soil fractions whereas silver shows little variation between the three size fractions. These relations indicate that the tin and tungsten are present in particulate cassiterite and wolframite whereas the silver is secondarily dispersed into precipitates from weathering processes in the soil. The geochemical profile for tungsten indicates significant anomalies in the middle of the profile (45+00 to 46+100 N) where mineralization was not encountered during mapping. This area is characterized by well-developed frost polygon structures and frost boils and the tungsten anomalies may represent significant tungsten mineralization in the bedrock below the soil cover. Cassiterite mineralized rock was found in the vicinity of 36+00 to 39+00 N and 57+00 to 60+00 N along the profile which accounts for the tin

Table 4. --Contrast in trace element content in various size fractions of soils

Element (fraction)	$\bar{x}^{\dagger}$	$\bar{x} \pm \sigma^{\dagger}$
Sn (-80 mesh)	128.7	228.6 - 28.8
Sn (-28+80 mesh)	340.5	478.5 - 202.5
Sn (-14+28 mesh)	359.5	621.5 - 97.5
W (-80 mesh)	22.2	46.7 - -2.3
W (-28+80 mesh)	84.9	166.7 - 3.1
W (-14+28 mesh)	38.3	93.1 - -16.5

†Note: all values in ppm (N=10)

anomalies in the soils at these locations.

The intent of this baseline survey was to examine anomaly definition and contrast at different size fractions. For each size fraction a calculation of the mean ($\bar{x}$) $\pm$ the standard deviation (σ), $\bar{x} \pm \sigma$, is used to compare the degree of contrast between the different size fractions, table 4. The range of $\bar{x} \pm \sigma$ for tungsten that exhibits the greatest contrast is the -28+80-mesh fraction. This is because the multiple that equates the

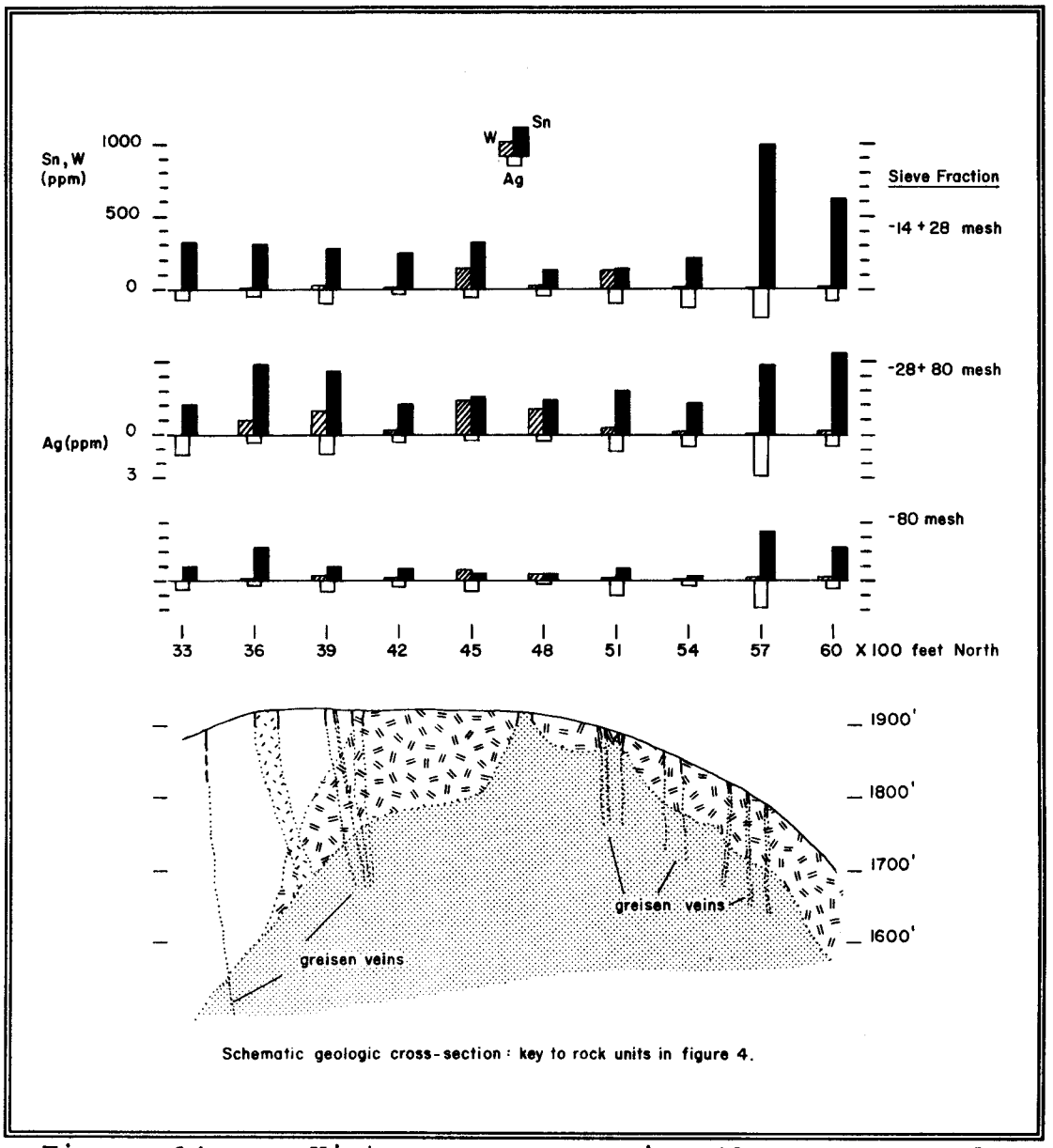

Figure 14. --Histograms expressing the Sn, W, and Ag content of -80-mesh, -28+80-mesh, and -14+28-mesh size fractions of soils along crossline 42+00 East.

lowest to the highest value is greatest for this fraction. Tin concentrations overall are greatly enhanced in the coarse soil fractions, however, little contrast is evident in the intermediate -28+80-mesh fraction. The contrast is similar between the coarse -14+28-mesh and the fine -80-mesh fractions but a higher level of detection can be obtained using the coarser fraction.

Pan Concentrate Survey

A methodical pan concentrate survey was conducted peripheral to the deposit in order to characterize the level of dispersion and level of anomalies a deposit of this morphology and magnitude would express. Routinely, one level 14-in. pan of -½-in. material was gathered from the top 1-2 ft of surface gravels in active drainages and panned to a weight of 40-70 g. A graphical representation of the data is presented as figure 15 and the analytical results are tabulated in appendix B.

The area sampled was not extensive, however, figure 15 shows that anomalous values (≈ >1,000 ppm) are confined to drainages that erode the Sleitat Mountain granite stock. Dispersion trains of anomalous tin in these drainages were not fully evaluated, but values of up to 5,200 ppm were found three miles downstream of the deposit. Drainages that do not include the stock, contain significantly less tin and this is evident in samples taken in the northeastern quadrant of figure 15.

CONCLUSIONS

A significant tin-mineralized granite containing an estimated 28.6 million st of greisen-altered granite grading 0.22-0.37 % tin occurs in an area largely devoid of magmatic rocks. The presence of this deposit invites speculation about the economic potential of the region when geologic models for tin deposits and regional geochemical and geophysical survey results are applied. The Sleitat Mountain stock is a multi-unit, highly differentiated, peraluminous, and altered granite. This specialized granite has trace element and mineralogic characteristics that indicate a history of emplacement followed by subsequent evolution of a hydrous phase to produce a zoned alteration pattern in the stock. These hydrothermal fluids caused extensive greisen alteration and mineralization along high-angle east-west-oriented fracture systems that extend to significant depths (>350 ft) below the present erosional surface.

Wallace and others (4) suggested that the Mulchatna fault is the northwestern limit of the Alaska Range magmatic belt (fig. 2), and that an area of magmatic quiescence exists between the Kuskokwim and Alaska Range belts. There appears, however, to be sufficient evidence to indicate that the Mulchatna Fault does not

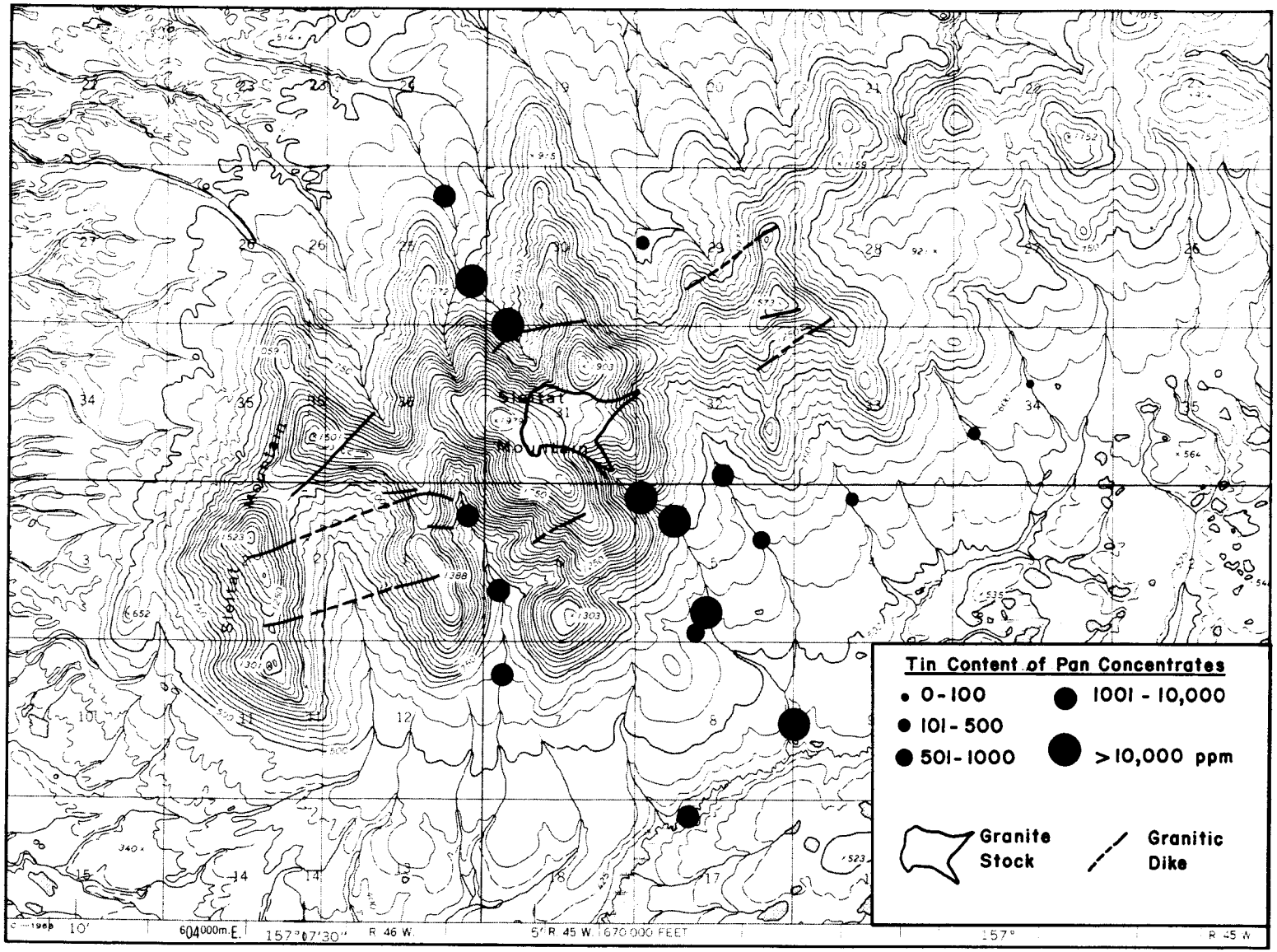

Figure 15. Graphic representation of tin concentrations of panned concentrate samples. Base map taken from USGS 1:63,360 scale Taylor Mtns A-3 & A-4 quadrangle maps.

present a structural boundary to latest Cretaceous-Paleocene magmatic activity in this region. The Tired Pup Pluton, a large, 760 square mile, 56 Ma, weakly peraluminous and moderately differentiated, locally tin-bearing granite batholith (25, 26, 27), is located just north of the Mulchatna Fault (fig. 2). Further to the southwest, King and others (28) identified significant tin anomalies from heavy mineral fractions of stream sediment samples at Halfway Mountain and in the hills just north of the Mulchatna fault at longitude 156° W (fig. 2). Interpretations of areomagnetic data by Case and Nelson (29) indicate contoured magnetic features that suggest unexposed intrusive bodies underlie these tin geochemical anomalies. This evidence also suggests that a magmatic continuum may exist between the Kuskokwim Mountains and Alaska Range belts and this interim region may be fertile ground for finding other partially exposed, or unexposed, tin-mineralized systems like Sleitat Mountain. The specialized geochemical characteristics of the Sleitat Mountain stock are comparable to other tin-producing granite-complexes of the world and should be applicable exploration criteria for tin-granites in the region.

REFERENCES

1. Carlin, J.F., Jr. Tin. in Mineral Commodity Summaries, 1990. Department of Interior, U.S. Bureau of Mines, Washington, D. C., 1990, pp. 178-179.

2. Warner, J.D. . Critical and Strategic Minerals in Alaska; Tin, Tantalum and Columbium. BuMines IC-9037, 1985, 19 pp.

3. Burns, L.E., and R. J. Newberry. Intrusive rocks of the Lime Peak - Mt. Prindle area, Part A: Tin-related Granites of the Lime Peak - Mt. Prindle Area. in Mineral Assessment of the Lime Peak - Mt. Prindle Area, Alaska. eds. T.E. Smith, G. H. Pessel and M.A. Wiltse. Vol. I., 1987, pp.3-1 - 3-83.

4. Wallace, W.K., C.L. Hanks and J.F. Rogers. The Southern Kahiltna Terrane; Implications for the Tectonic Evolution of Southwestern Alaska. Geol. Soc. America Bull., v. 101, 1989 , pp. 1389-1407.

5. Bundtzen, T.K., and W. G. Gilbert. Outline of Geology and Mineral Resources of Upper Kuskokwim Region, Alaska. Journal of the Alaska Geological Society, 1983, pp. 101-117.

6. Wallace, W.K. and D.C. Engebretson. Relationships Between Plate Motion and Late Cretaceous to Paleogene Magmatism in Southwestern Alaska. Tectonics, v. 3., no. 2, 1984, pp. 295-315.

7. Farnstrom, H.E.. (Cominco Alaska Exploration). Private Communication, 1990.

8. Hudson, T. and J.G. Arth. Tin Granites of Seward Peninsula, Alaska. Geological Society of America Bulletin, v. 94., 1983 pp. 768-790.

9. Taylor, R.G. Geology of Tin Deposits. New York, Elsevier Scientific Publishing Co., 1979, 543 pp..

10. Manning, D.A.C., and P.I. Hill. The Petrogenetic and Metallogenetic Significance of Topaz Granite from the Southwest England Orefield. Geological Society of America Special Paper 246, in press.

11. Thorton, C.P., and O.F. Tuttle. Chemistry of Igneous Rocks, I, Differentiation Index. American Journal of Science, v. 258, 1960, pp. 664-684.

12. Tischendorf, G.. Geochemical and Petrographjic Characteristics of Silicic Magmatic Rocks Associated with Rare-element Mineralization. in Stemprok M., Burnol, B. and Tischendorf, B. eds., Symposium, Metallization Associated With Acid Magmatism. Prague, Czechoslovakia, Geological Survey, v. 2, 1977, pp. 41-96.

13. Swanson, S.E., Bond, J.F., and R.J. Newberry. Petrogenesis of the Ear Mountain Tin Granite, Seward Peninsula, Alaska. Economic Geology, vol. 83., 1988, pp.46-61..

14. McCarthy, T.S. and R.A. Hasty. Trace Element Distribution Patterns and Their Relationship to the Crystallization of Granitic Melts. Geochimica et Cosmochimica Acta, vol. 40, 1976, pp. 1351-1358.

15. Alderton, D.H. A., Pearce, J.A., and J.A. Potts. Rare Earth Element Mobility During Granite Alteration: Evidence from South-west England. Earth and Planetary Science Letters. vol. 40, 1980, pp. 149-165.

16. Collins, W.J., Beams, S.D., White, A.J.R., and B.W. Chappell. Nature and Origin of A-type Granites with Particular Reference to Southeastern Australia. Contributions to Mineralogy and Petrology. vol. 80, 1980, pp. 189-200.

17. Hill, P.I. and D.A.C. Manning. Multiple Intrusions and Pervasive Hydrothermal Alteration in the St Austell Granite, Cornwall. Proceedings of the Usher Society 6, 1987, pp. 447-453.

18. Faure, G. and J.L. Powell. Strontium Isotope Geology. Springer-Verlag, New York, 1972, 188 p.

19. Lanphere, M.A., and B.L. Reed. The McKinley Sequence of Granitic Rocks: A Key Element in the Accretionary History of Southern Alaska. Journal of Geophysical Research, 1985, vol. 90, pp. 11,413-11,430.

20. Robinson, M.S., Nye, C., and J. Decker. Preliminary Whole Rock Major Oxide and Trace Element Geochemistry of Selected Igneous Rocks from the Sleetmute, Russian Mission, and Taylor Mountains Quadrangles, Southwestern Alaska. Public Data File 86-98, 1986, Alaska Division of Mining and Geological and Geophysical Surveys. 5 p.

21. Lehmann, B.. Metallogeny of tin: Magmatic Differentiation Versus Geochemical Heritage. Econ. Geol., v. 77, 1982, pp. 50-59.

22. Heinrich, C.A.. The Chemistry of Hydrothermal Tin(-Tungsten) Ore Deposition. Econ. Geol., v. 85, 1990, pp.457-481.

23. Breiner, S.. Magnetics: Applications for Portable Magnetometers. in Practical Geophysics for the Exploration Geologist, R.V. Blaricom, compiler. Northwest Mining Association, Spokane, Wa. 1980, pp 205-238.

24. Fraser, D.C.. Contouring of VLF-EM Data. Geophysics, vol. 34, no. 6, 1969, pp. 958-967.

25. Reed, B.L., and M.A. Lanphere. Alaska-Aluetian Range Batholith: Geochronology, Chemistry, and Relation to Circum-Pacific Plutonism. Geological Society of America Bulletin, v. 84, 1973, pp. 2583-2610.

26. Reed, B.L. and T.P. Miller. Uranium and Thorium Content of Some Tertiary Granitic Rocks in the Southern Alaska Range. USGS Open-file Report 80-1052. 1980, 16 pp.

27. Burleigh, R.E. Field Report on Tin Exploration of the Tired Pup Pluton in the Little Underhill Creek Drainage, Southwest Alaska. Unpublished field report of the U.S. Bureau of Mines, Alaska Field Operations Center(AFOC) - Fairbanks, Alaska. 1990, 23 pp.. Available upon request from AFOC-Fairbanks, Ak.

28. King, H.D., R.B. Tripp, E.F. Cooley, and W.D. Crim. Maps Showing the Distribution and Abundance of Selected Elements in Two Geochemical Sampling Media, Lake Clark Quadrangle, Alaska. USGS Map MF-1114C, 1985, four sheets.

29. Case, J.E., and W.H. Nelson. Maps Showing Areomagnetic Survey and Geologic Interpretation of the Lake Clark Quadrangle, Alaska. USGS Map MF-1114E, 1986, two sheets.

APPENDIXES

Appendix A. Data for the soil sample profile in figure 13.

Grid Location	Sieve size	Sn, ppm	W, ppm	Ag, ppm
33+00 N	-14 to +28	320	2	.7
	-28 to +80	205	8	1.3
	-80	100	4	.5
36+00 N	-14 to +28	315	4	.4
	-28 to +80	490	100	.6
	-80	230	6	.3
39+00 N	-14 to +28	285	35	.9
	-28 to +80	440	170	1.3
	-80	100	45	.8
42+00 N	-14 to +28	250	4	.3
	-28 to +80	205	35	.5
	-80	80	10	.4
45+00 N	-14 to +28	320	150	.5
	-28 to +80	260	230	.4
	-80	49	80	.7
48+00 N	-14 to +28	13	23	.3
	-28 to +80	235	185	.3
	-80	44	35	.2
51+00 N	-14 to +28	140	130	1.0
	-28 to +80	300	55	1.2
	-80	88	10	1.0
54+00 N	-14 to +28	220	18	1.2
	-28 to +80	225	28	.8
	-80	36	3	.4
57+00 N	-14 to +28	1000	4	2.0
	-28 to +80	480	5	2.9
	-80	335	16	1.9
60+00 N	-14 to +28	615	13	.7
	-28 to +80	565	33	.8
	-80	225	13	.5

Note - Tin analysis by XRF, tungsten by carbonate sinter - colourimetric and silver by HNO_3-HCl hot extraction - atomic absorption methods.

Appendix B. Analytical data for pan concentrate and soil samples.

Map Number	Sample Number	Sn ppm	W ppm	Ag ppm
1	KS27158A	85	<2	1.2
	KS27158B	100	2	<2.0
	KS27158C	35	<2	1.0
2	KS27159A	38	2	.1
	KS27159B	35	2	.2
	KS27159C	14	2	.1
3	KS27173A	135	<2	.2
	KS27173B	79	<2	.5
	KS27173C	9	<2	<.1
4	KS27017	*56300	8200	1.7
5	KS27018	*18700	8100	1.7
6	KS27020	*56300	6300	1.2
7	KS27021	925	105	.2
8	KS27022	*43000	3200	.4
9	KS27023	5200	250	<.1
10	KS27156	*2400	400	<.1
11	KS27157	*400	100	<.1
12	KS27170	*300	100	<.1
13	KS27171	*5000	100	.1
14	KS27172	*300	100	<.1
15	KS27174	2600	650	.3
16	KS27175	2600	1000	.5
17	KS27176	3400	2300	1.3
18	KS27195	*4000	1200	.6
19	KS27196	680	55	.1
20	KS27197	190	18	<.1
21	KS27198	96	6	<.1
22	KS27225	*29300	8600	2.7
23	KS27226	*41300	8100	2.4
24	KS27227	690	260	.1
25	KS27228	2300	400	.4
26	KS27229	300	23	.5
27	KS27230	385	75	1.0

Note - Tin analysis by XRF, tungsten by carbonate sinter - colourimetric and silver by HNO_3-HCl hot extraction - atomic absorption methods. An asterisk (*) denotes tin assay by peroxide fusion - atomic absorption methods.